Nanoelectronics Beyond Si: Challenges and Opportunities

Prof. J. Raynien Kwo 郭瑞年
國立清華大學

Si CMOS Device Scaling – Beyond 22 nm node
High κ, Metal gates, and High mobility channel

1947 First Transistor

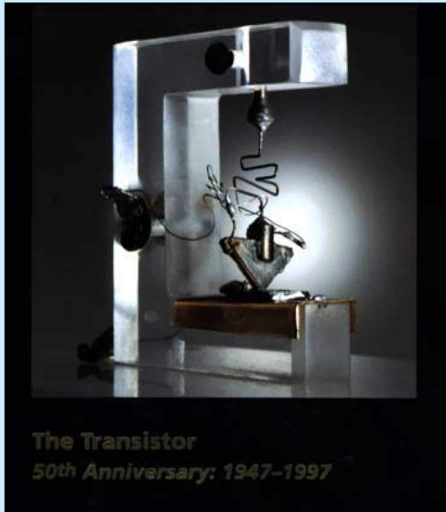

1960 First MOSFET

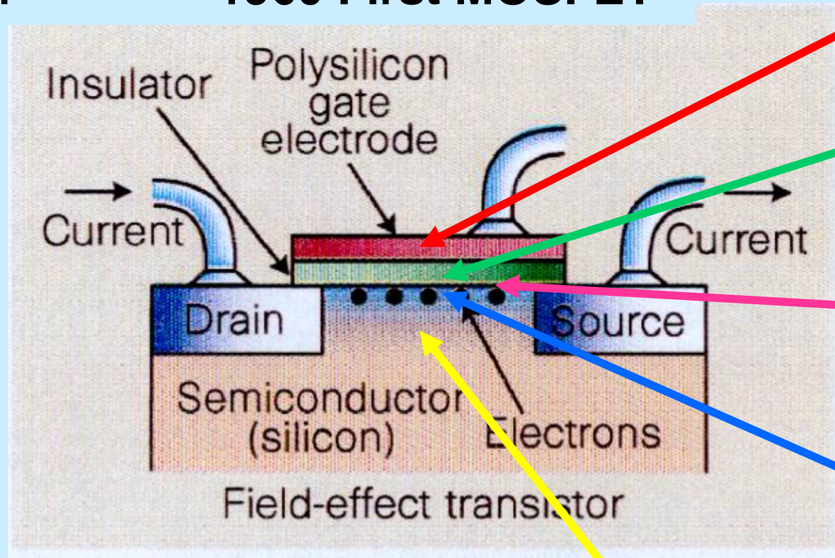

Moore's Law: The number of transistors per square inch doubles every 18 months

Shorter gate length *L*
Thinner gate dielectrics t_{ox}

Driving force :
High speed
Low power consumption
High package density

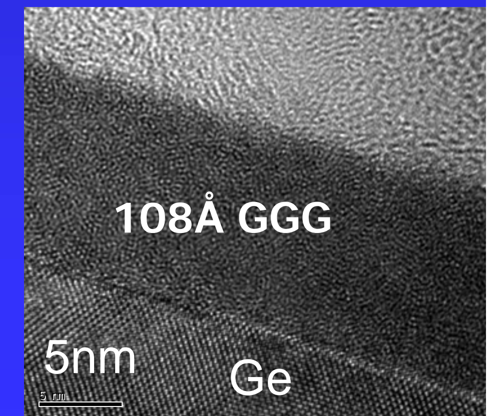

Intel Transistor Scaling and Research Roadmap

Ultimate scaling of CMOS

(22 nm node and beyond)

More non-silicon elements introduced

2013-2019

90nm Node
2003

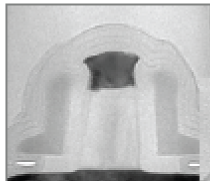

(Production)

65nm Node
P1264
2005

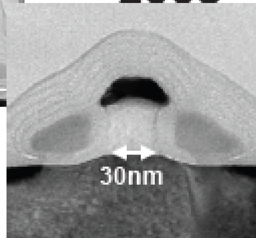

(Development)
(production)

45nm Node
P1266
2007

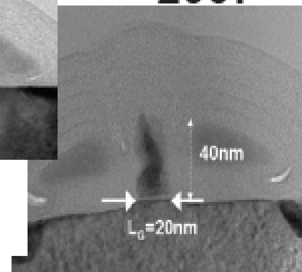

(production-early2008)
(Development)

32nm Node
P1268
2009

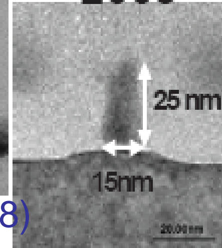

(development)
(Research)

22nm Node
P1270
2011

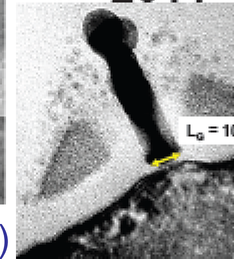

(Research)

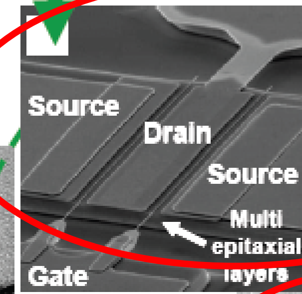

III-V Device
Prototype
(Research)

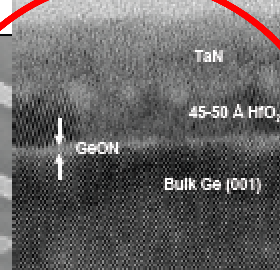

C-nanotube
Prototype
(Research)

Ge Device
Prototype
(Research)

Uniaxial
Strain

SiGe S/D

High-K/
Metal-Gate

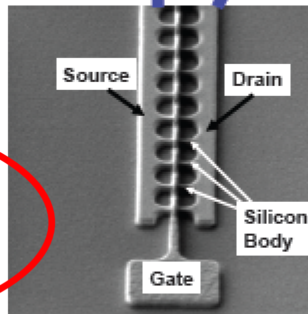

Tri-Gate
Architecture

Major Research Subjects

- Enhancement of κ in the new phase through epitaxy
- Fundamental study by IETS for detections of phonons and defects in high κ dielectrics
- Room temperature ferromagnetism in cluster free, Co doped HfO_2 films

Can you make κ even higher ?

" Phase Transition Engineering"

---Enhancement of κ in the New Phase through Epitaxy

Crystal structures of HfO_2 and the corresponding κ

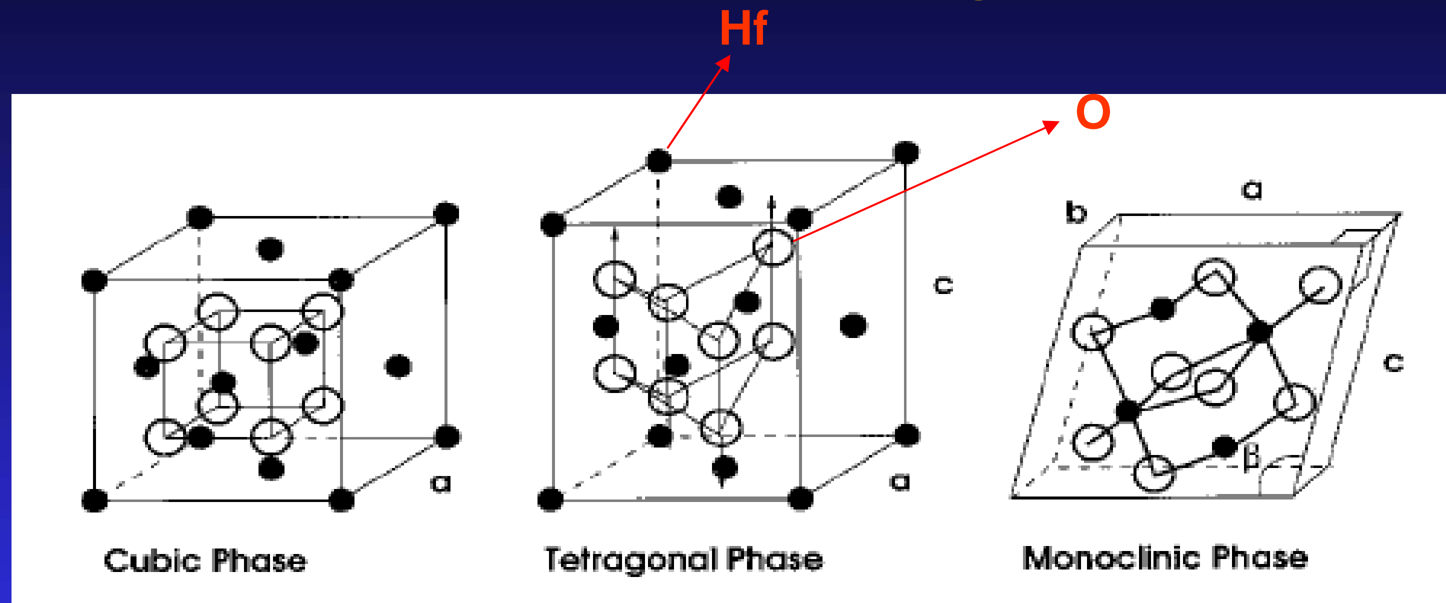

	Cubic	Tetragonal	Monoclinic
Dielectric constants	*29*	*70*	*16 **
Stable phase temperature	*>2700°C*	*>1750°C*	*<1750°C*

The dielectric constant increases when HfO_2 structure is changed from monoclinic to other symmetry

* Xinyuan Zhao and David Vanderbrit, P.R.B. 65, 233106, (2002).

Permittivity Increase of Yttrium-doped HfO_2 Through Structural Phase Transformation

by Koji Kita, Kentaro Kyuno, and Akira Toriumi, Tokyo Univ.

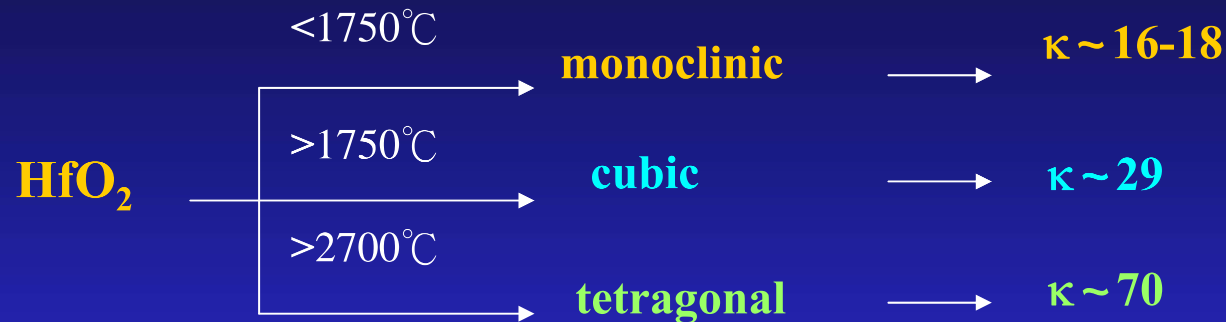

- Yttrium serves effectively as a dopant to induce a phase transformation from the ***monoclinic*** to the ***cubic*** phase even at 600 °C.
- Yttrium-doped HfO_2 films show higher permittivity than undoped HfO_2, and the permittivity as high as 27 is obtained by 4 at. % yttrium doping.
- The permittivity of undoped HfO_2 is reduced significantly at high temperature, whereas that of 17 at. % yttrium-doped film shows no change even at 1000 °C.

2x position

1x position

After deposition for 5mins

Dielectric film of 4 –fold symmetry in the plane

190 °

280 °

After deposition for 2mins

190 °

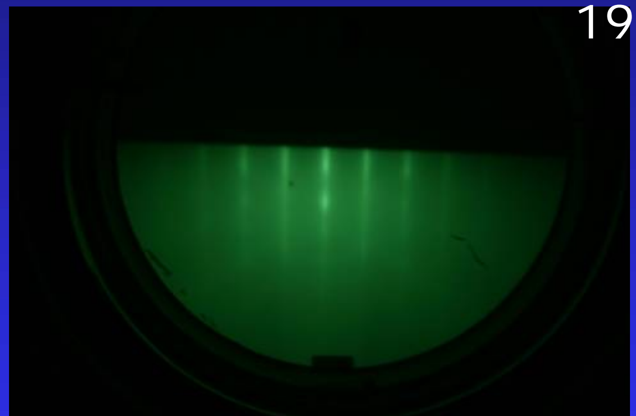

280 °

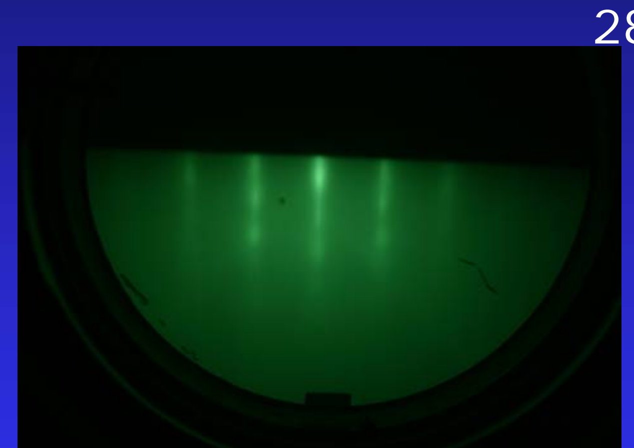

Wafer rotate22.5 °

After reconstruction

145 °

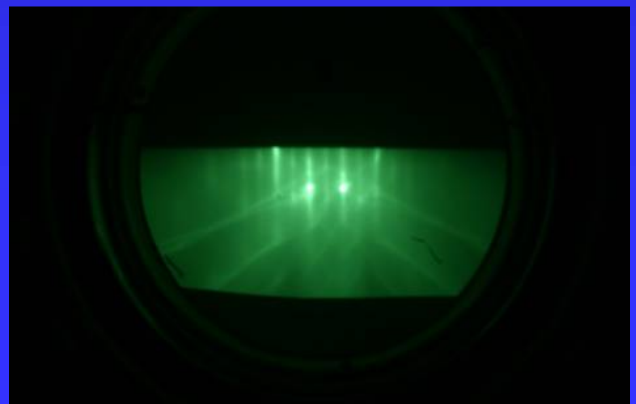

235 °

HRTEM of Low Temp Growth

Amorphous HfO_2 on GaAs (100)

A very abrupt transition from GaAs to HfO_2 over one atomic layer thickness was observed.

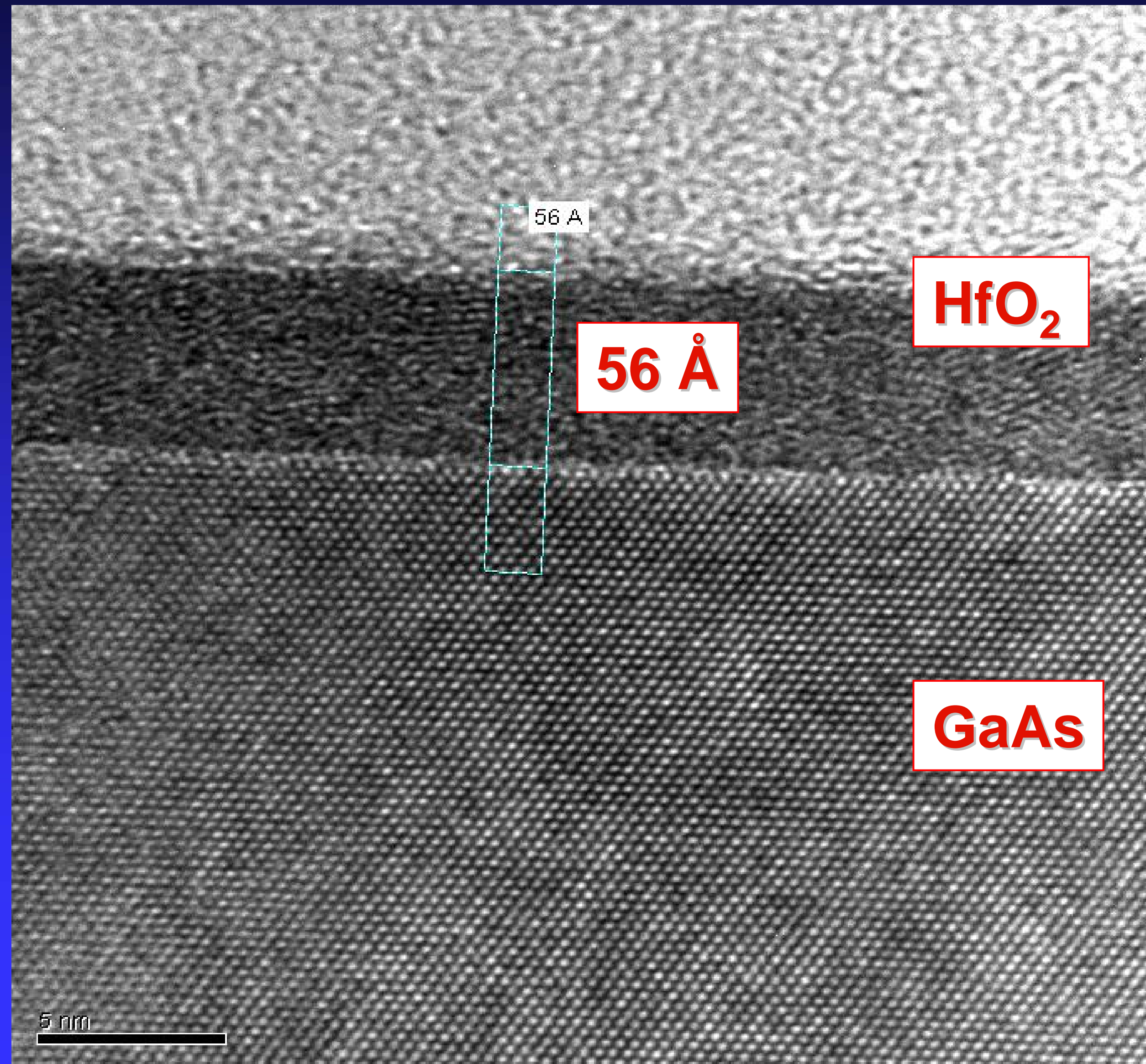

High Resolution TEM Images of Pure HfO_2 on GaAs (001)

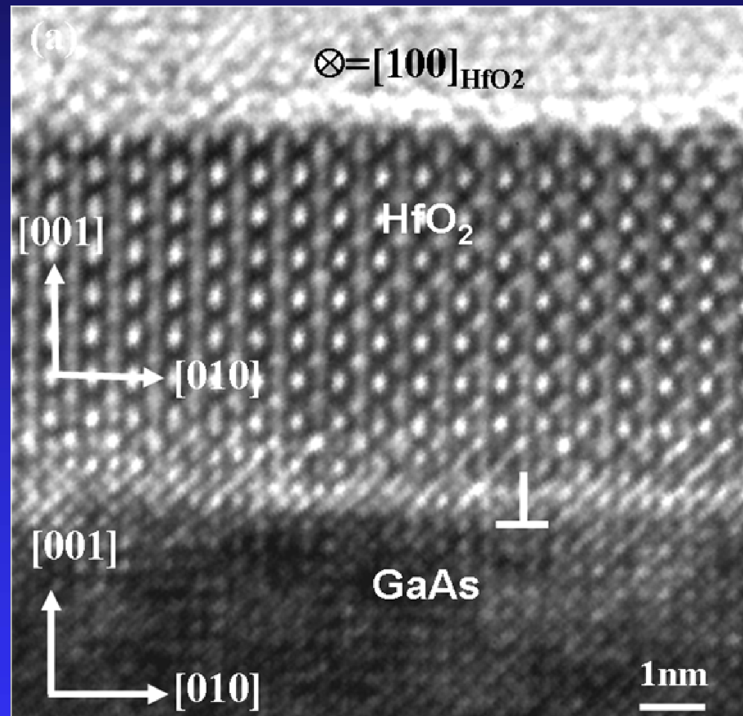

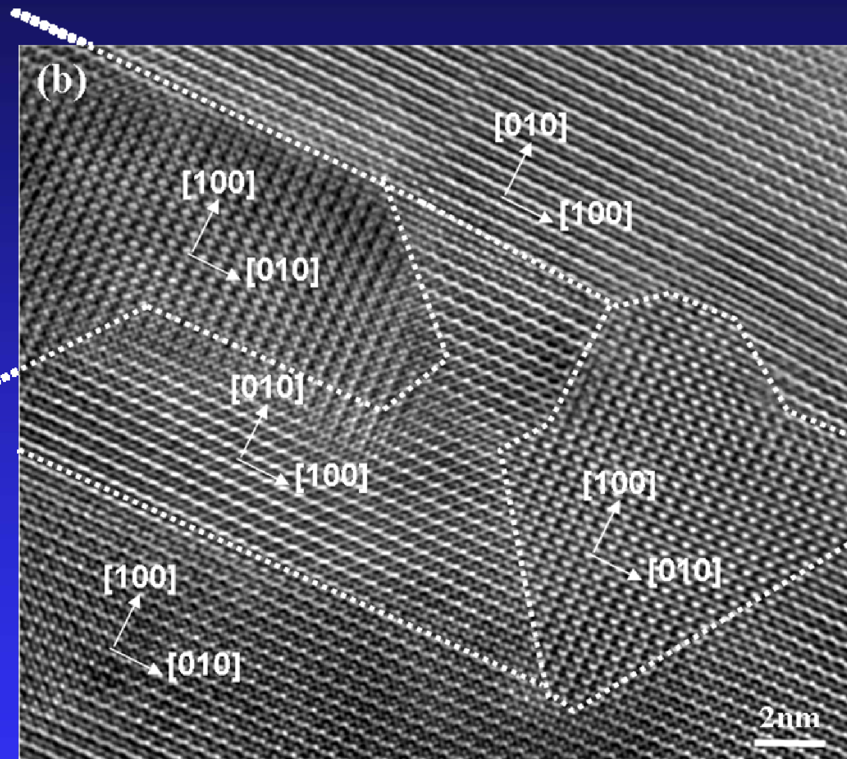

An abrupt transition from GaAs to HfO_2 and no interfacial layer

Coexistence of four monoclinic domains rotated by 90º.

X-ray Diffraction of Epitaxial HfO_2 Films Recrystalized on GaAs

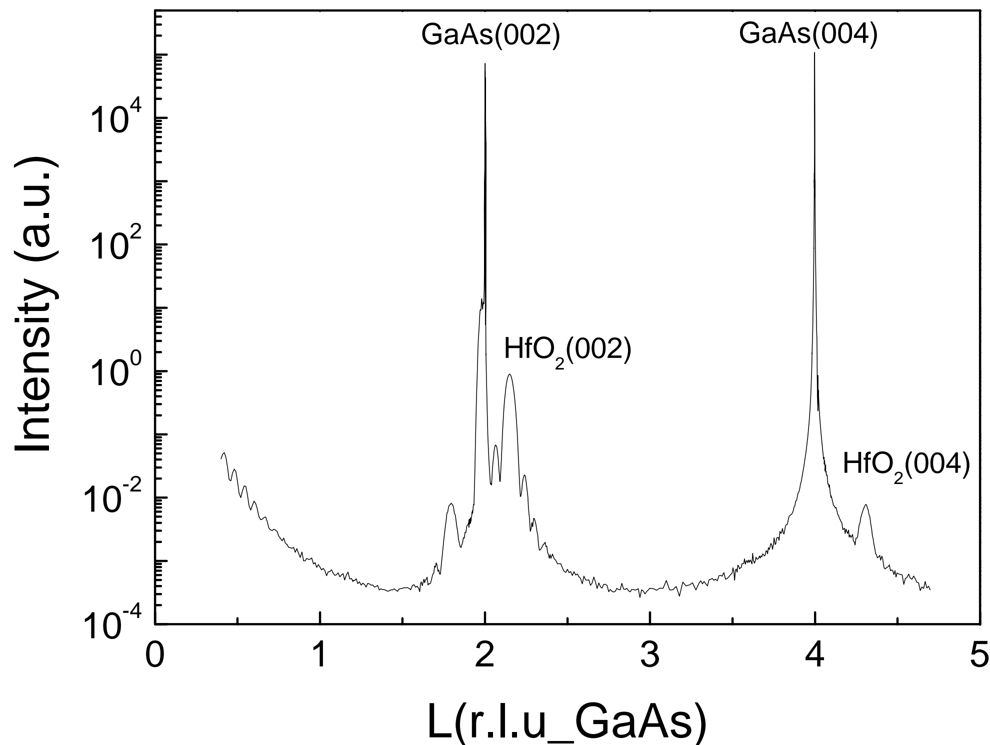

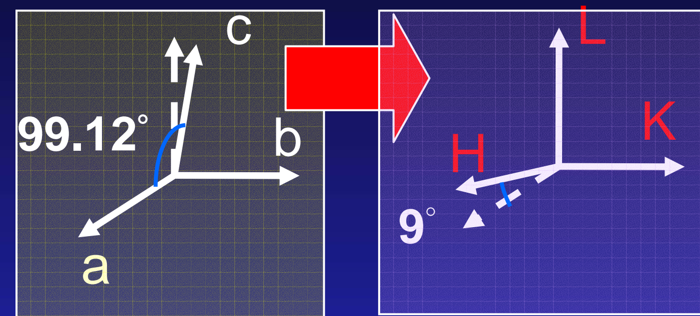

R space

K space

--- Monoclinic HfO_2 in R space and K space
--- Forming four degenerate domains about the surface normal

With C. H. Hsu of NSRRC

HfO_2(004) FWHM(L)=0.0578°
⇒ domain size 97.8 Å
⇒ close to film thickness

The Structure of HfO_2 Grown on GaAs(001)

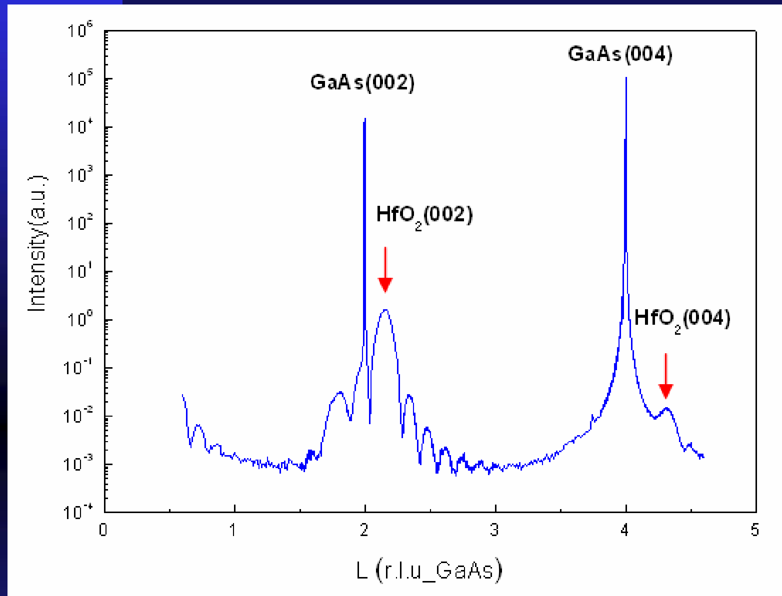

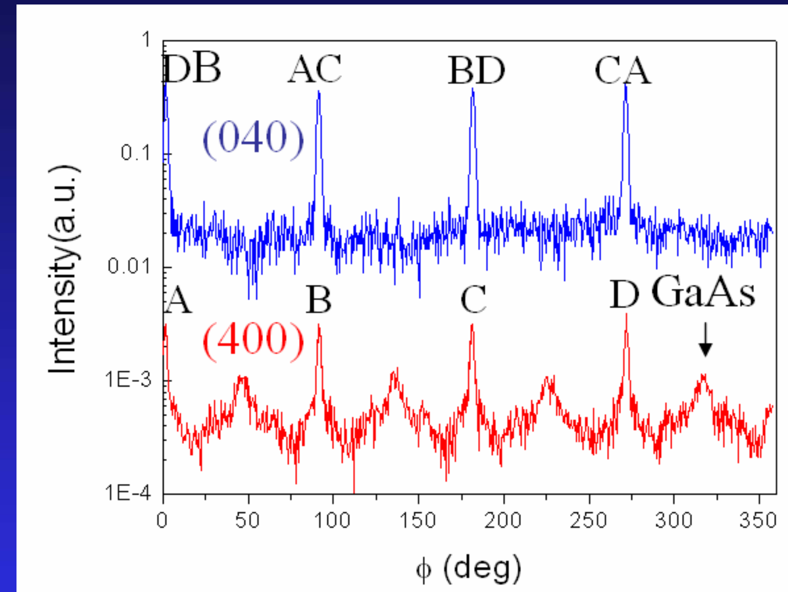

monoclinic phase

a=5.116A, b=5.172A, c=5.295A, β=99.18A

Coexistence of 4 domains rotated 90° from each other

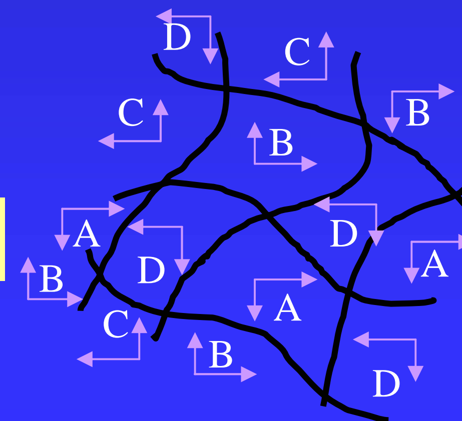

The Structure of HfO_2 doped with Y_2O_3 Grown on GaAs (100)

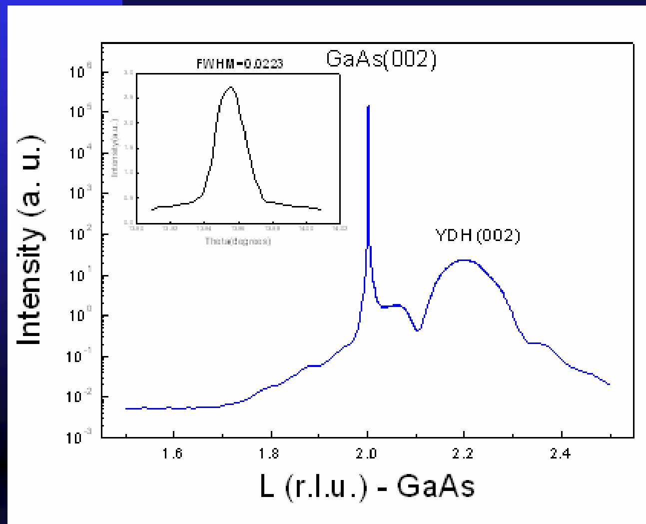

Surface normal scan

Find the peaks:

- (022)(400)(200)(311)(31-1)(113)(420)(133)(20-2)
- All peaks of film match the JCPDS of cubic phase HfO_2
- Use the d-spacing formula to fit the lattice parameters

→ HfO_2 doped with Y_2O_3 Grown on GaAs(001) is

Cubic phase

a=5.126A, b=5.126A, c=5.126A

α =90, β =90, γ =90

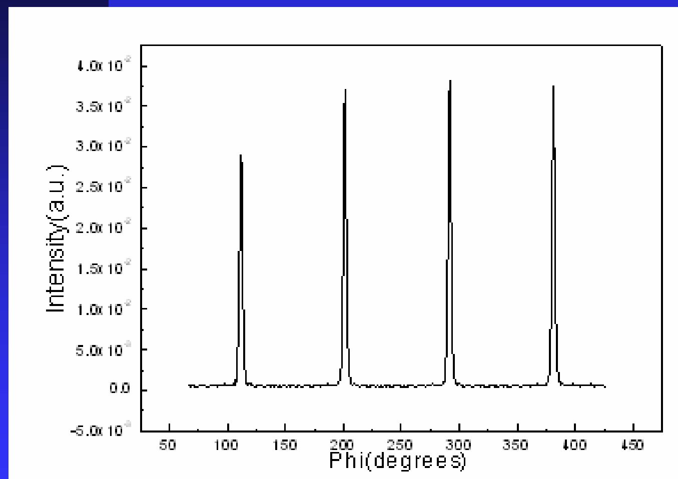

(400)Phi scan

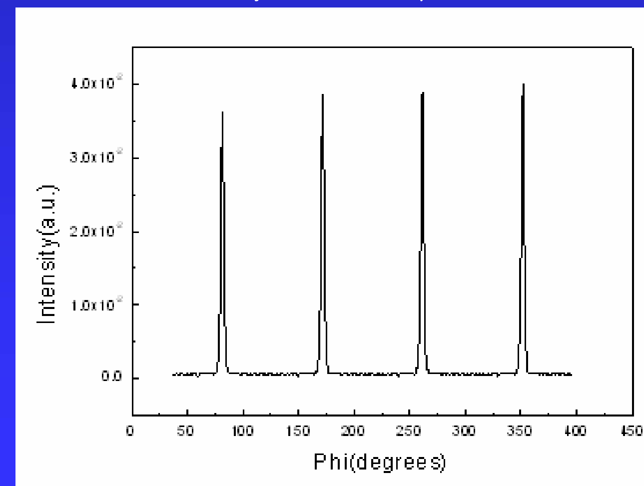

(040)Phi scan

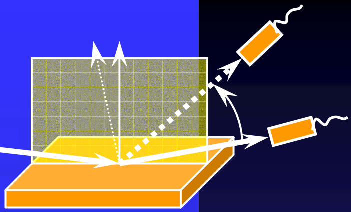

Comparison between Monoclinic phase and Cubic phase of HfO_2

Without doping Y_2O_3

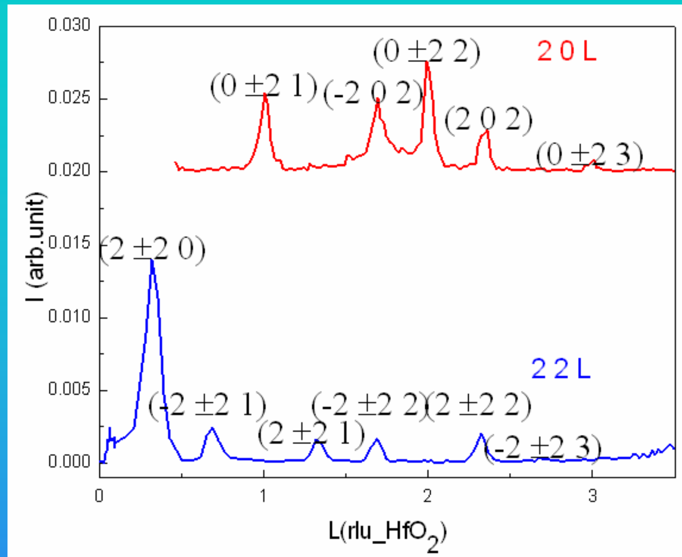

200 & 220 L scan

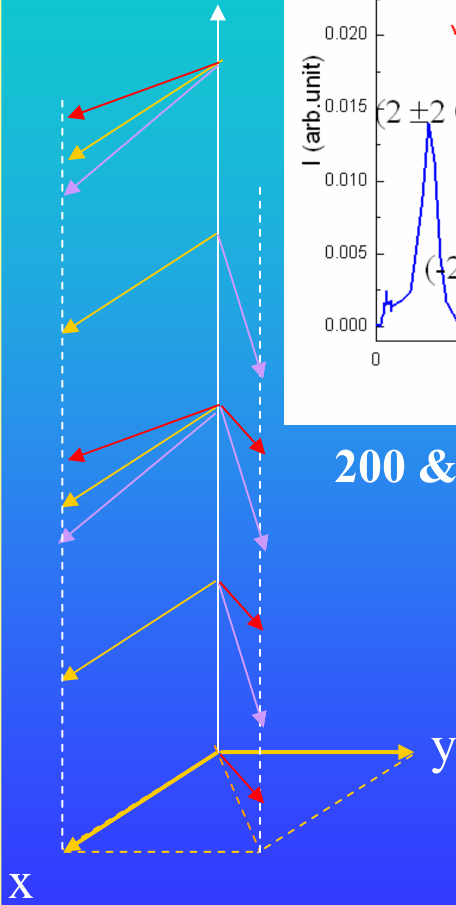

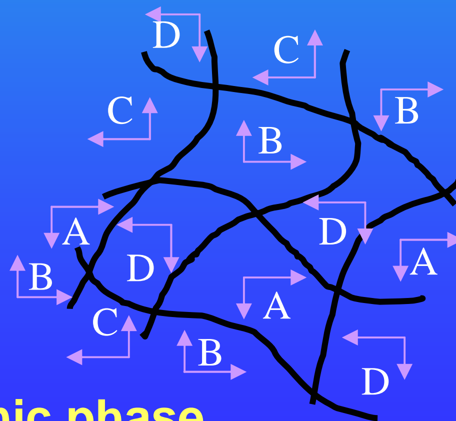

Monoclinic phase

With doping Y_2O_3

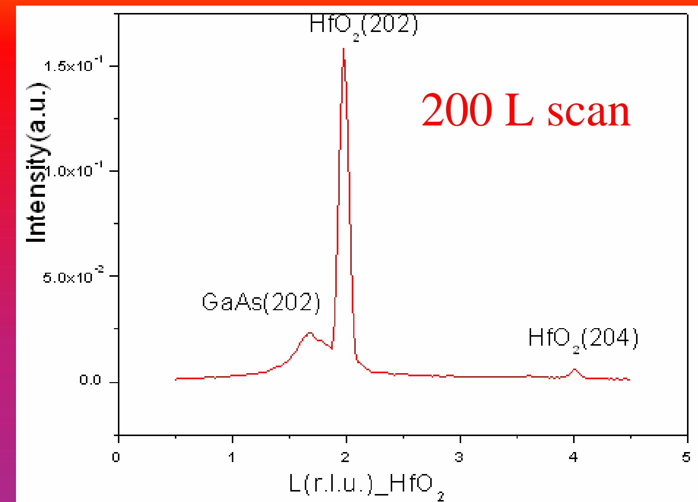

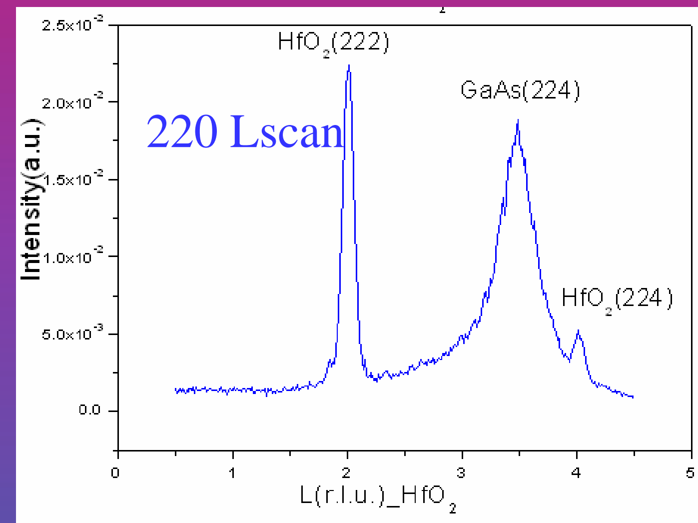

Cubic phase

The Electrical Property of HfO_2 doped with Y_2O_3 Grown on GaAs(001)

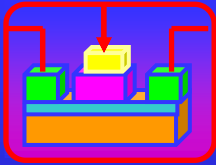

T=110A κ=32

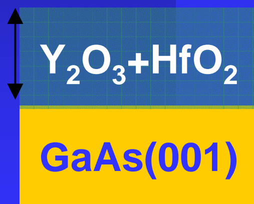

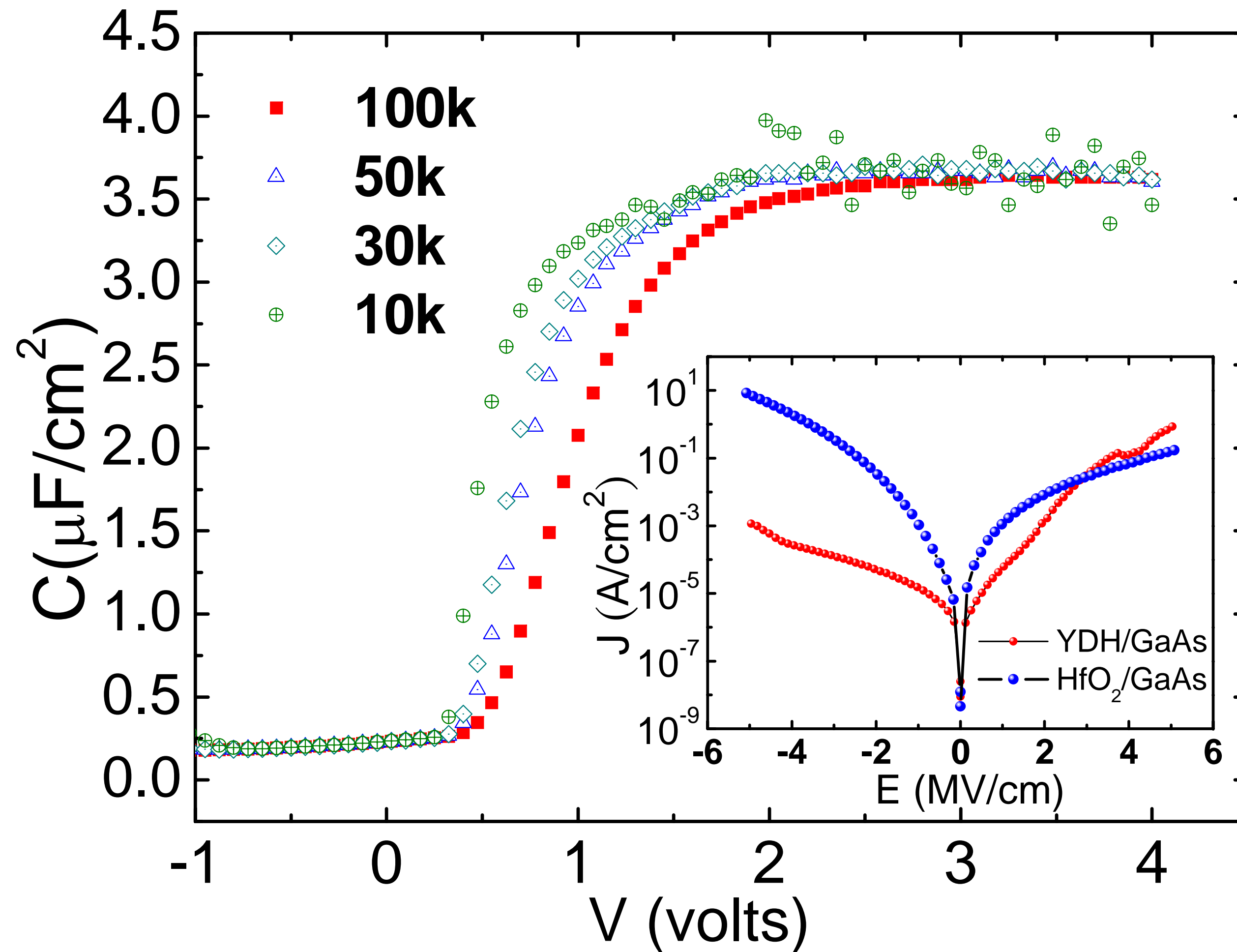

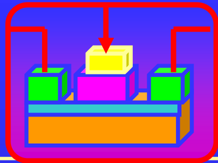

Electrical properties - MBE-$HfO_{2\,(0.8)}$ /$Y_2O_{3\,(0.2)}$

MBE-$HfO_{2\,(0.8)}$ /$Y_2O_{3\,(0.2)}$

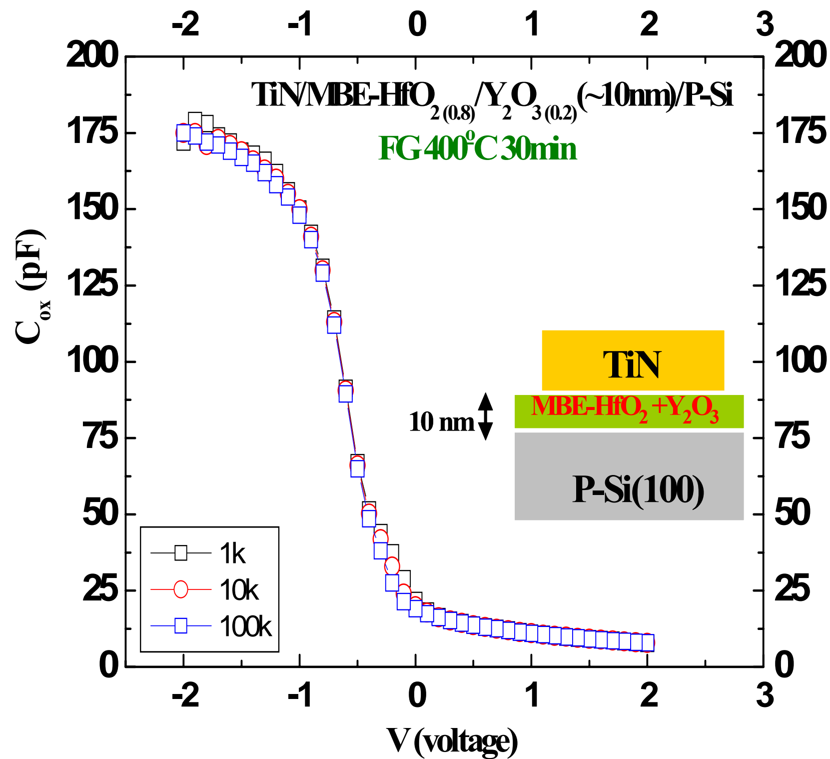

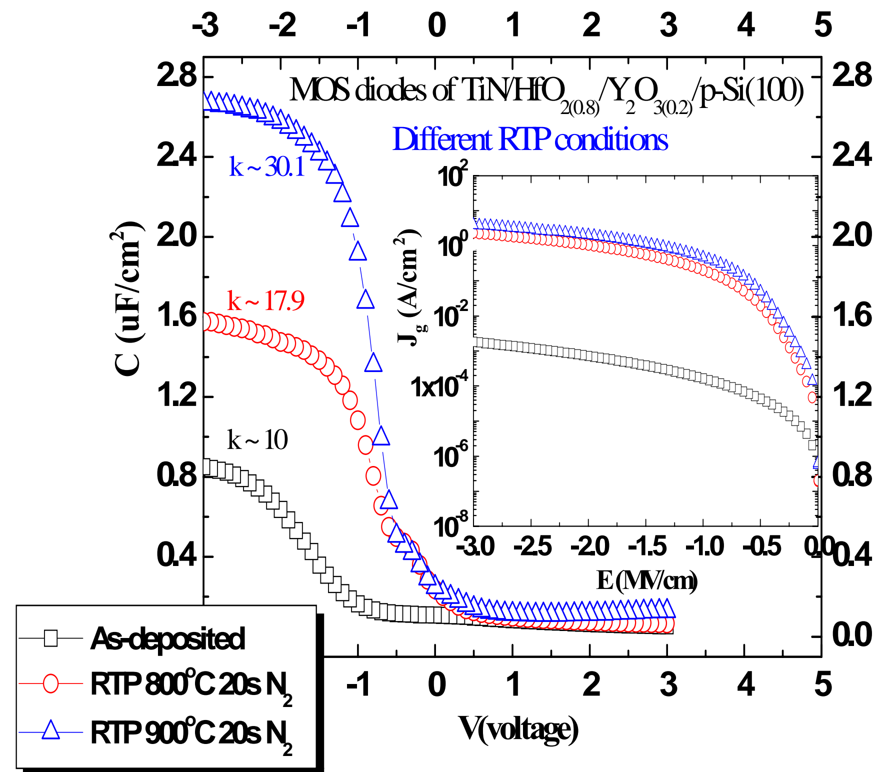

Increase of κ from 15 to over 30 in cubic phase !

Cross Sectional HRTEM Study of The Y-doped HfO_2 Films in Cubic Phase

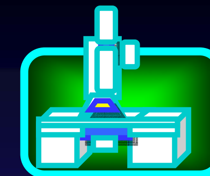

Interfaces of YDH(100)/GaAs, and YDH(111)/Si are atomically sharp

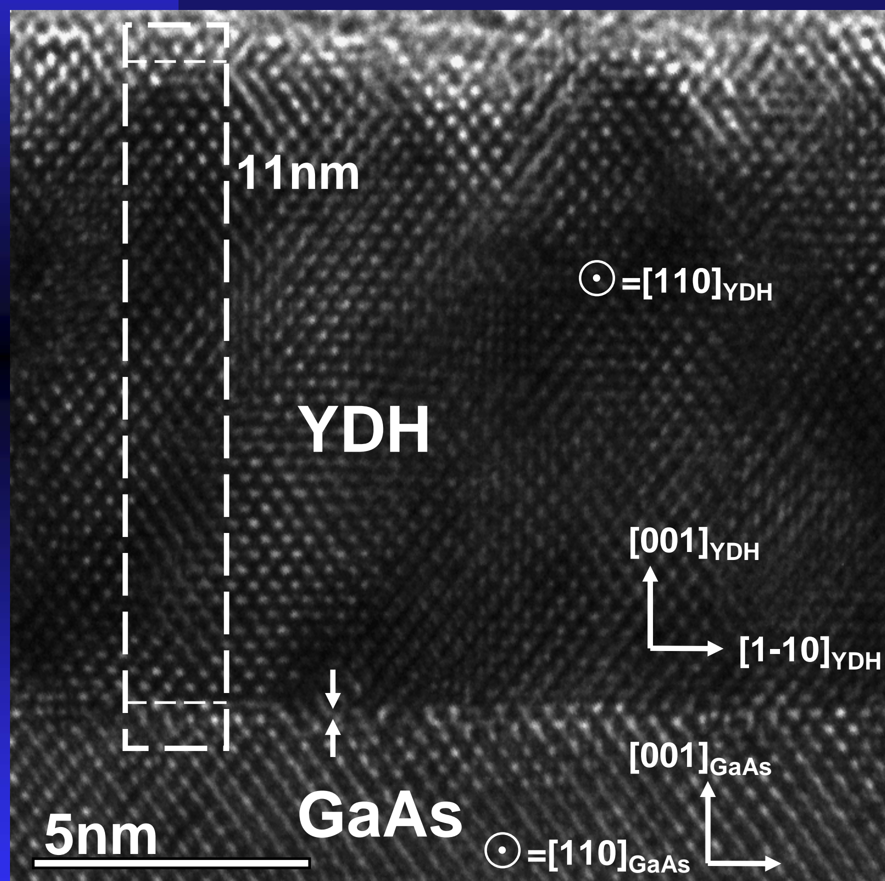

HRTEM image of yttrium-doped HfO_2 films 11 nm thick on GaAs (001).

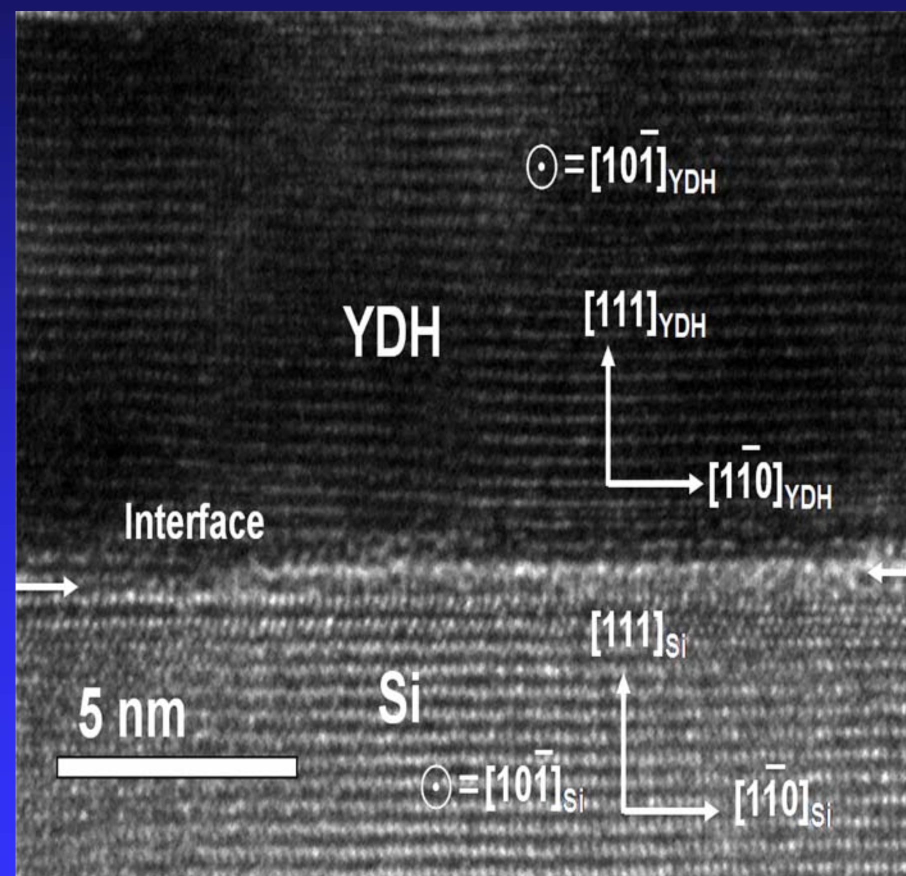

HRTEM image of yitturm-doped HfO_2 films 7.5 nm thick on Si (111).

The Enhancement of κ through "Phase Transition Engineering"

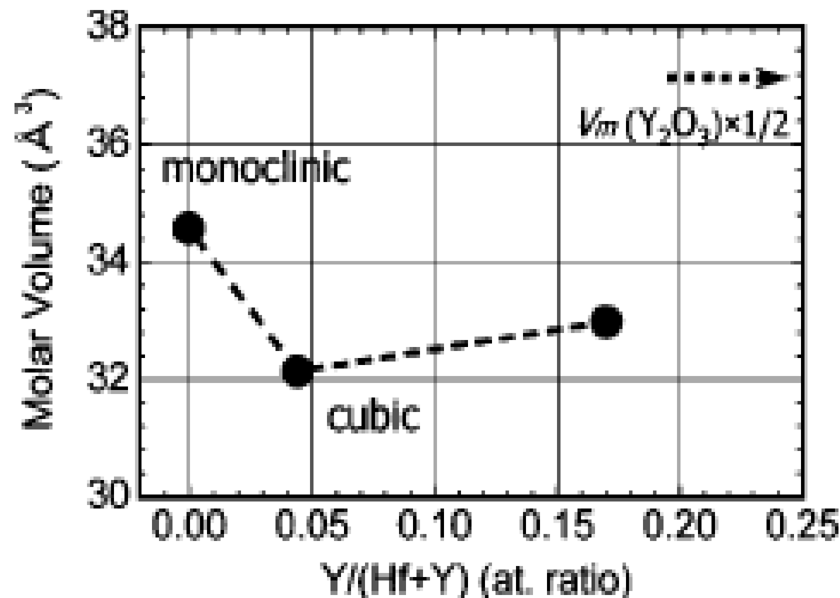

$$\kappa = (1 + 8\pi\, \alpha_m / 3V_m) / (1 - 4\pi\alpha_m / 3V_m)$$

Clausius-Mossotti Relation

Change of molar volume in Y doped HfO_2

- Many high κ materials, such as HfO_2, ZrO_2, TiO_2, Ta_2O_5, commonly have high temperature phases with a higher κ.
- Achieve the enhancement through ***phase transition engineering*** by additions of dopants such as lower valence cations, followed by proper post high temperature anneals.

IETS Study to Detect

Phonons and Defects in High κ Dielectrics

But what is inside of high κ ?

Electrical characterization / optimization

-- Good News !!

- **Low electrical leakage is common .**
- **Have Attained an EOT under 1.0-1.4 nm .**

-- Major problems are :

- High interfacial state density
- Large trapped charge
- Low channel mobility
- Electrical stability and reliability

Degradation of Mobility in High κ Gate Stack

Temperature dependence of mobility

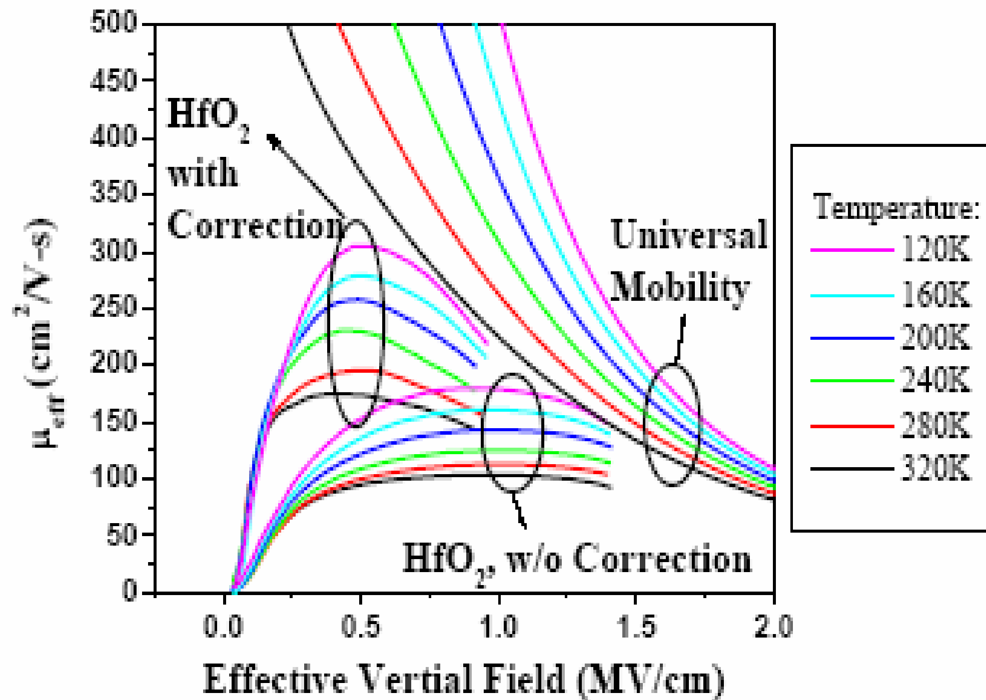

Correction from the charge trapping effect

- Effective mobility for HfO_2 is lower than universal mobility even after interface correction.

Phonons may have reduced mobility seriously !

Fechetti et al, JAP **90**, 4587, (2001).

Possible Source of Mobility Degradation

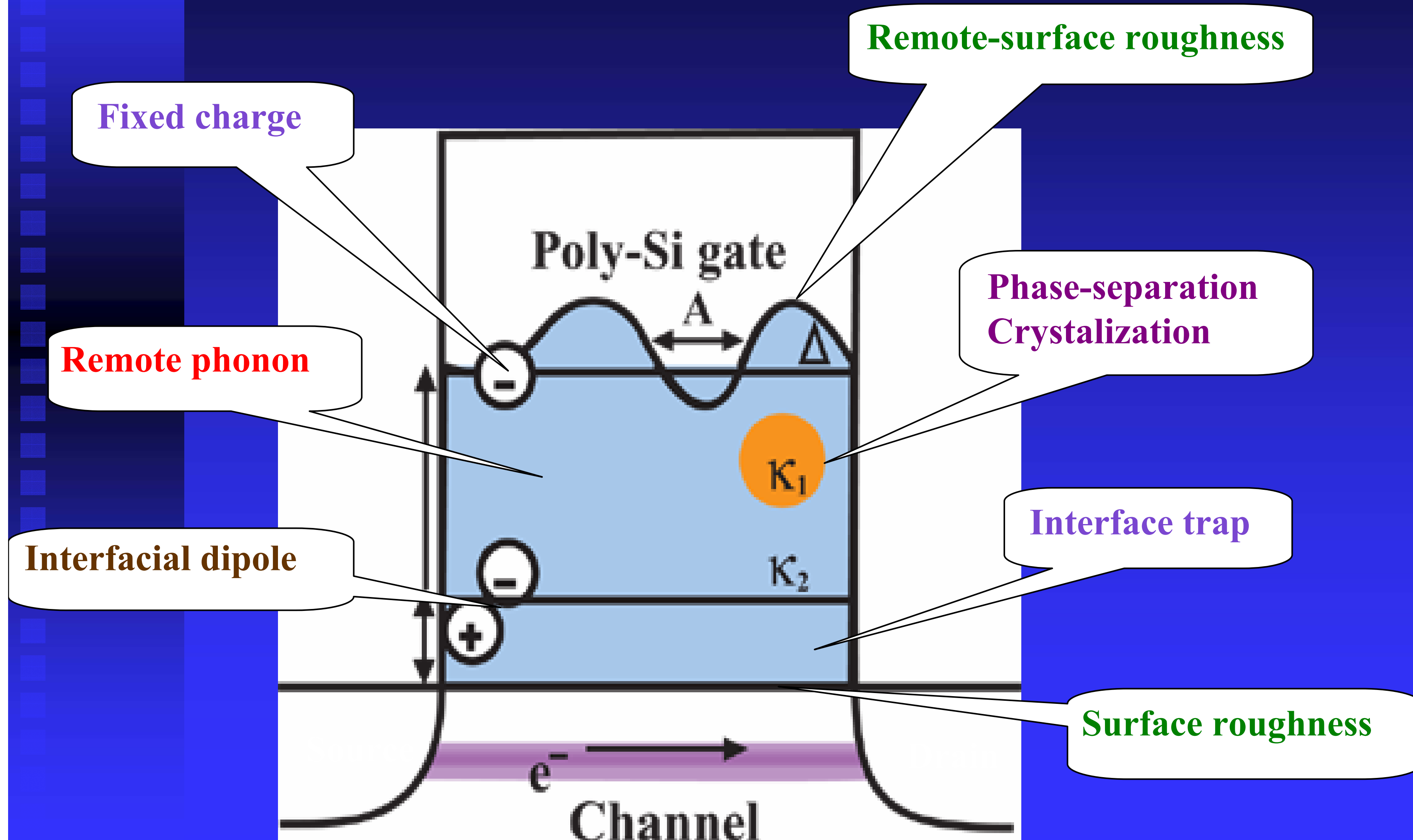

Interactions Detectable by IETS

- Substrate Silicon Phonons
- Gate Electrode Phonons
- Dielectric Phonons
- Chemical Bonding
- Interfacial Structures
- Defects (Trap States)

Trap-Related Signatures in IETS

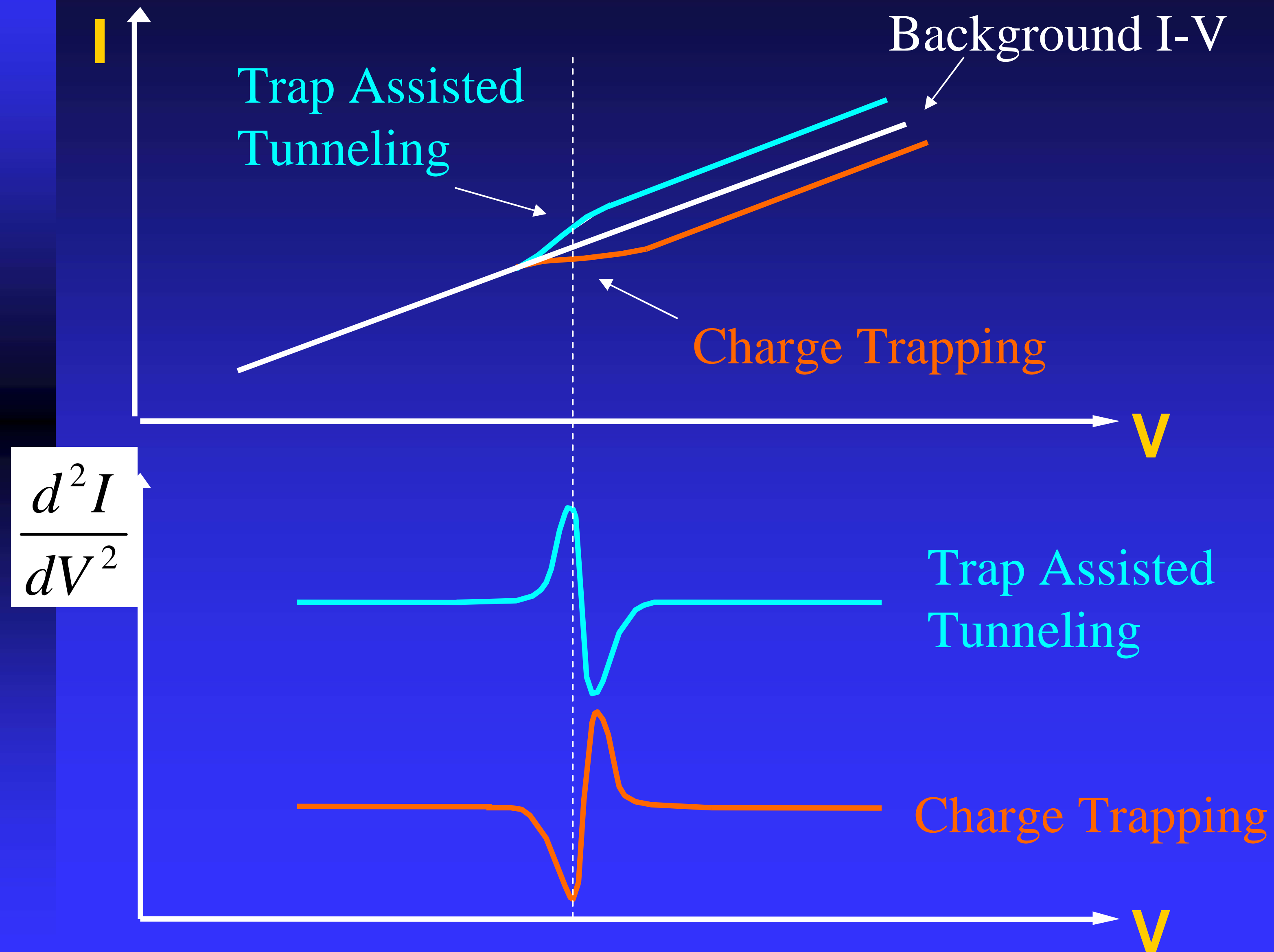

Wei He and T.P.Ma, APL **83**,2605, (2003) ; APL **83**, 5461, (2003).

Inelastic Electron Tunneling Spectroscopy (IETS)

Charge trapping will cause shift in the threshold voltage.

Trap-assisted conduction will cause increased leakage current.

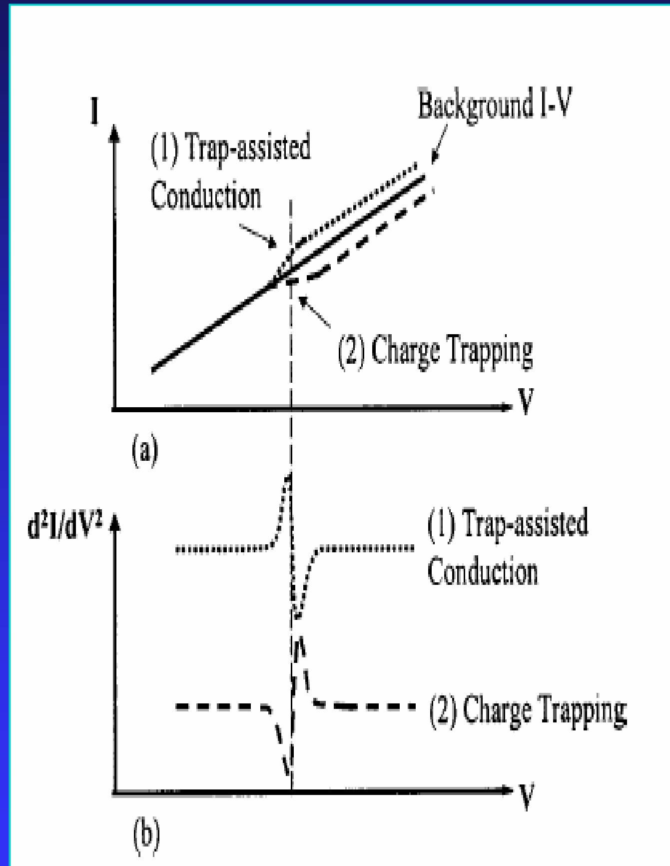

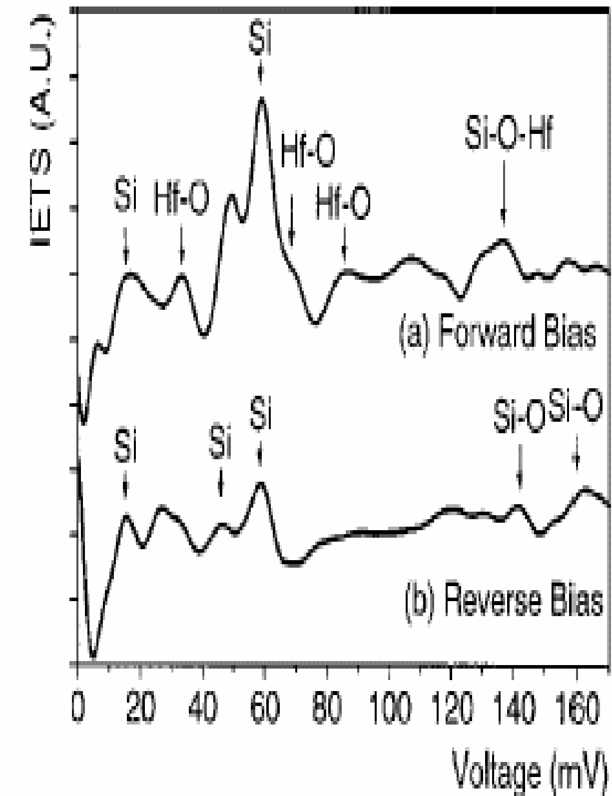

Wei He and T.P.Ma, APL **83**,2605, (2003) ; APL **83**, 5461, (2003)

IET spectrum of Al/HfO_2/Si MOS structure

Al/HfO_2/Si, vacuum 600℃ annealing for 3 minutes

d^2I/dV^2 (Arbitrary Units)

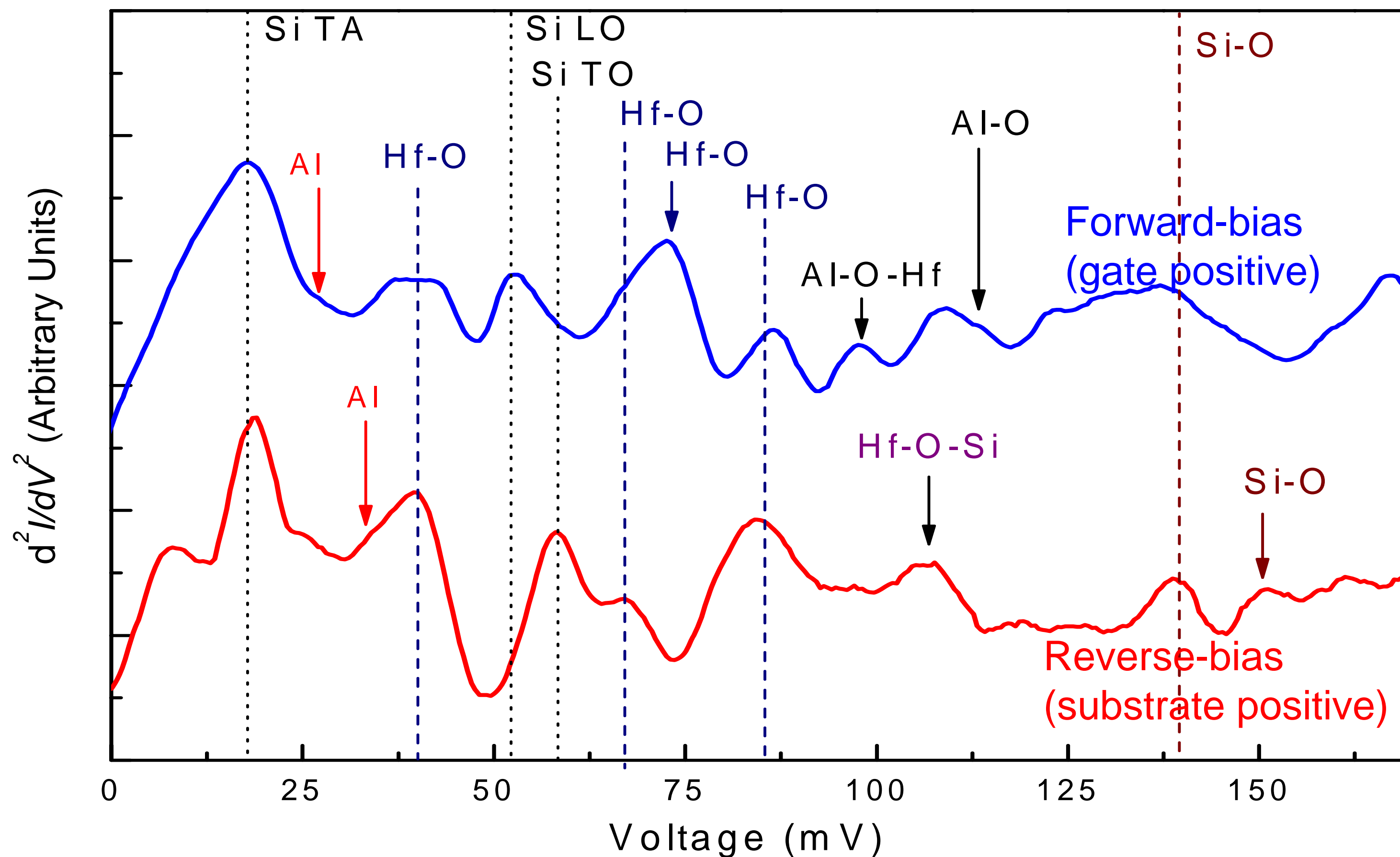

IET spectrum of Al/HfO_2/Si MOS structure

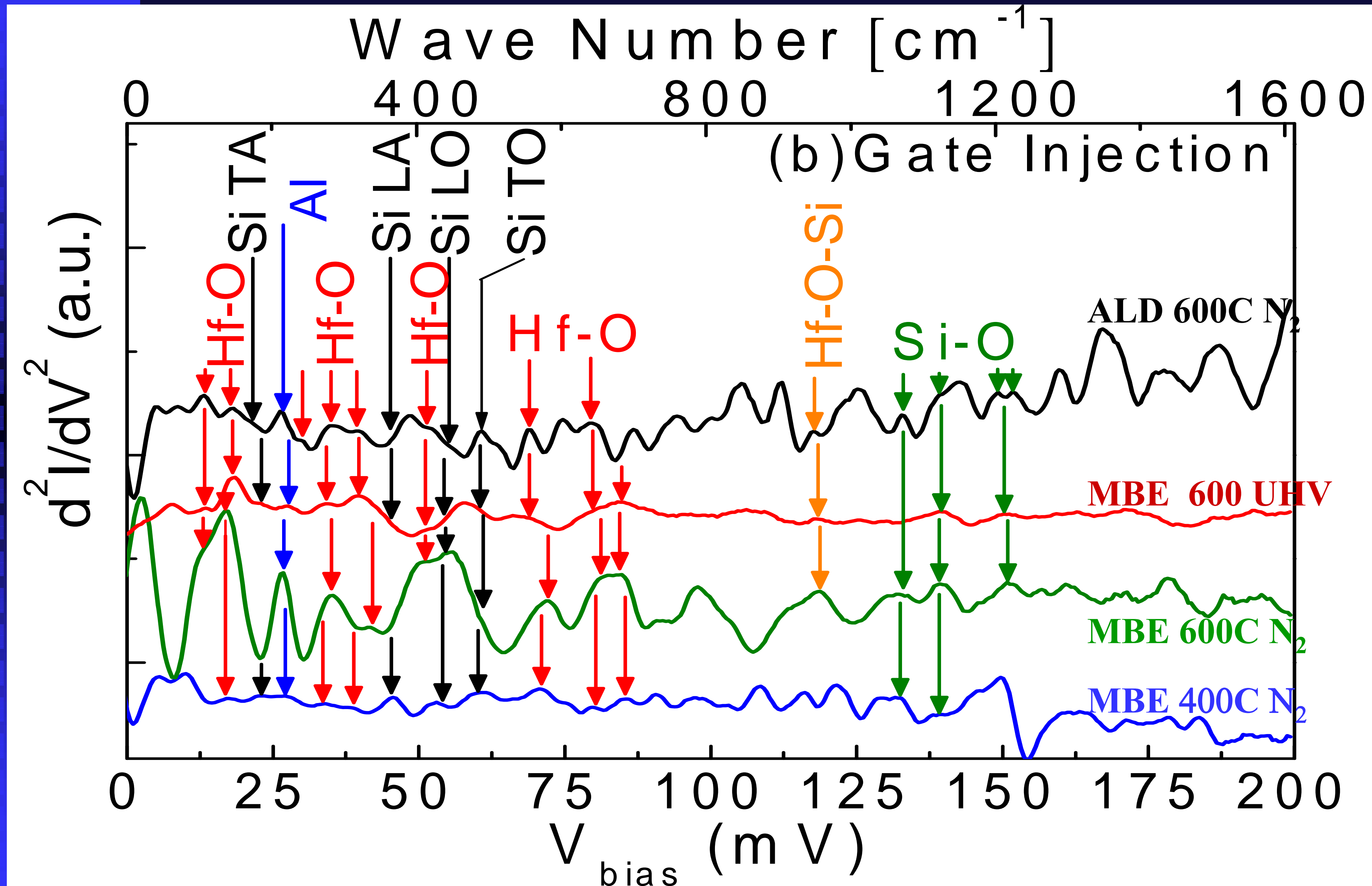

Monoclinic HfO_2

IET spectrum of Al/HfO2/Si MOS structure

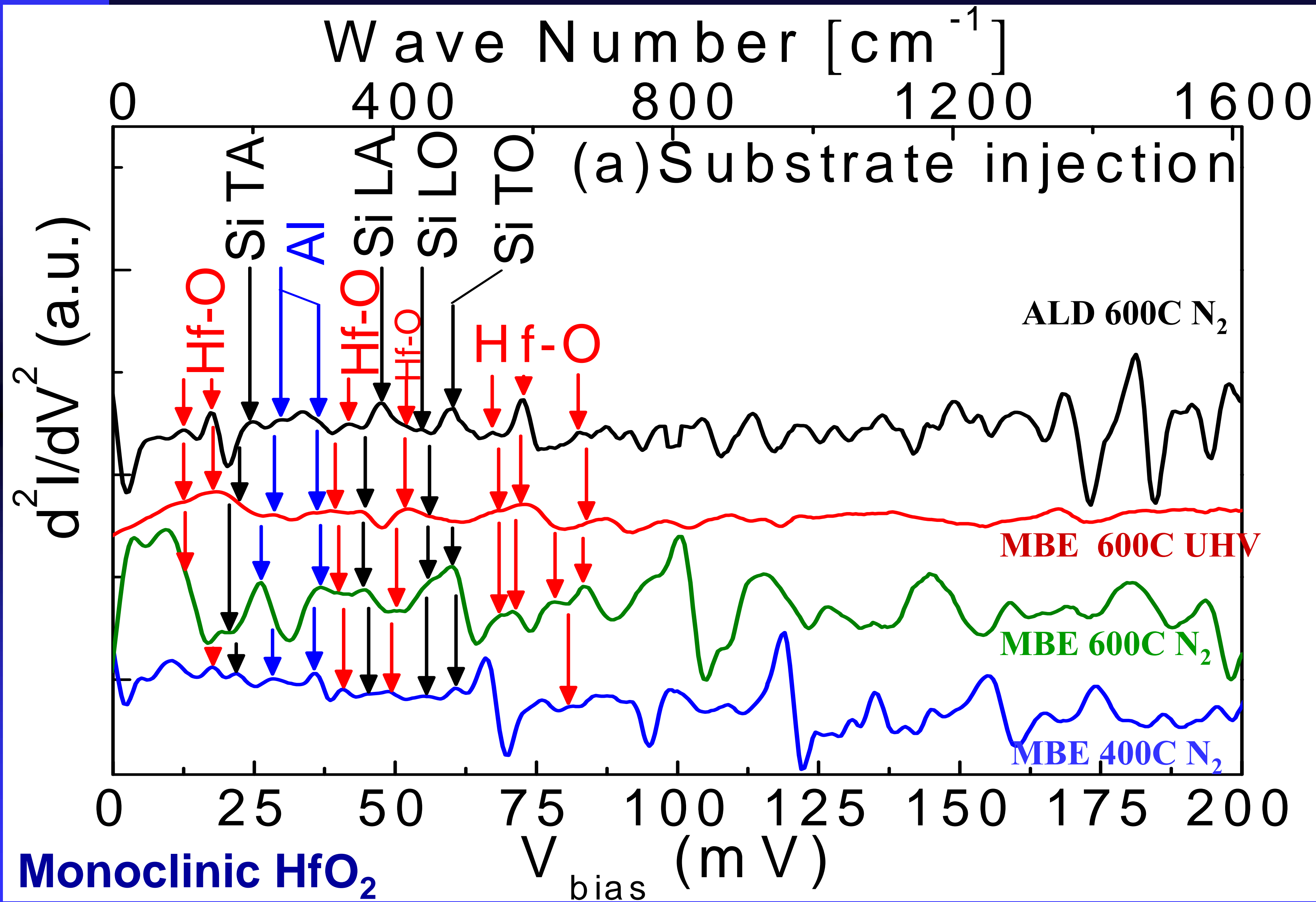

IET Spectrum of $Al/Y_2O_3/Si$ MOS Diode

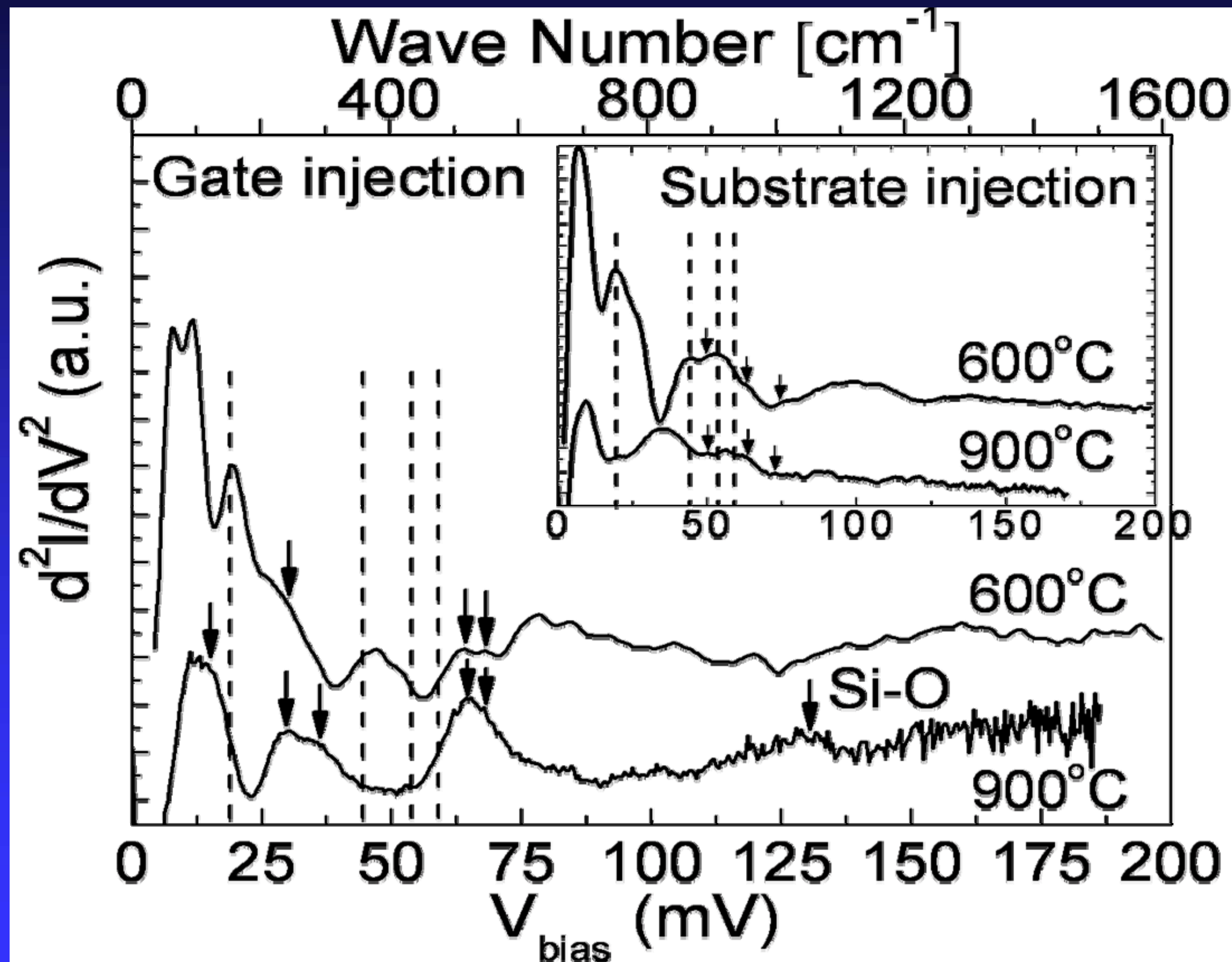

Cubic Y_2O_3

Determination of Physical Locations and Energy Levels of Trap in Stacked $HfO_2/Y_2O_3/Si$ Structure

Charge trapping

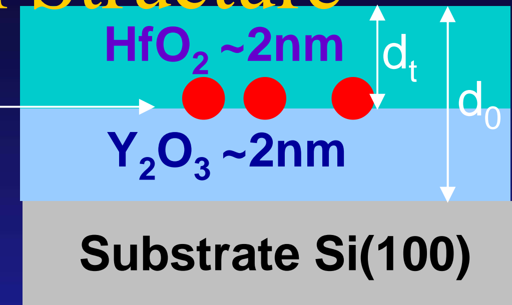

post-deposition annealing at
400 °C
600 °C
in N_2 ambiance for 3 min

HfO2~ 2nm
Y2O3~ 2nm
Si (100) Substrate

Si

d^2I/dV^2 (a.u.)

V_{bias} (mV)

$$\begin{cases} V_t = V_f V_r / (V_f + V_r) \\ d_t = d_0 V_f / (V_f + V_r) \end{cases}$$

V_f and V_r are the voltages where the charge trapping features occur in forward bias and reverse bias.

M. Wang et al,
APL. **86**, 192113 (2005)
APL, **90**, 053502 (2007)

Determination of Physical Locations and Energy Levels of Trap in Stacked $HfO_2/Y_2O_3/Si$ Structure

Bilayer Sample	Trap label	V_f (mV)	V_r (mV)	V_t (mV)	d_t/d_0
HfO_2(1.7nm) /Y_2O_3(1.4nm) 400°C	1	60	66	31	0.47
	2	67	75	35	0.47
	3	97	112	52	0.46
	4	118	135	63	0.46
HfO_2(1.7nm) /Y_2O_3(1.4nm) 600°C	5	58	66	31	0.46
	6	78	93	42	0.45
	7	103	124	56	0.45
	8	111	135	61	0.45
	9	120	148	66	0.45
HfO_2(1.2nm) /Y_2O_3(1.5nm) 600°C	1	26	32	14.3	0.45
	2	87	94	45.2	0.48
	3	99	108	51.7	0.48

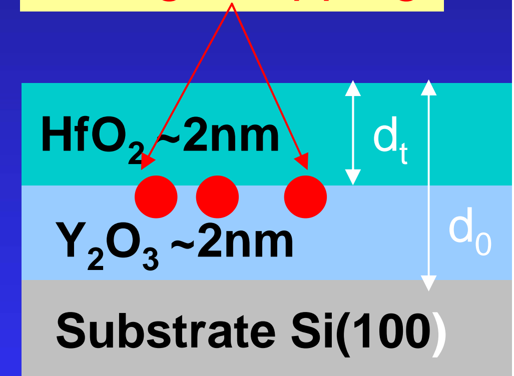

Can you make HfO_2 magnetic ?

Diluted Magnetic Oxides

"Observation of Room Temperature Ferromagnetic Behavior in Cluster Free, Co doped HfO_2 Films"

Appl. Phys. Lett. 91, 082504 (2007)

Introduction and motivation

- Both injection and transport of spin-polarized carriers are necessary for the spintronic devices. Using diluted magnetic semiconductor (DMS) as the ferromagnetic contact is one way to achieve this goal.
- Several models such as Zener's model, bound magnetic polaron, and F-center theory were used to describe the ferromagnetism.
- The potential usage of HfO_2 as alternative high-κ gate dielectrics in replacing SiO_2 for nano CMOS.
- Giant magnetic moment in Co doped HfO_2 as reported recently.

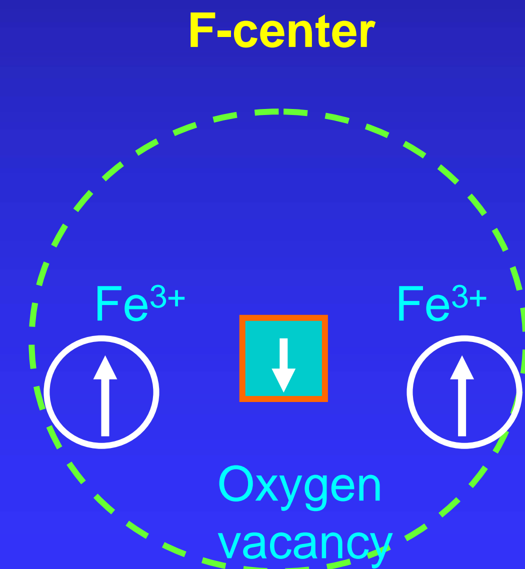

HR-TEM Images of High-T and Low-T Grown Films

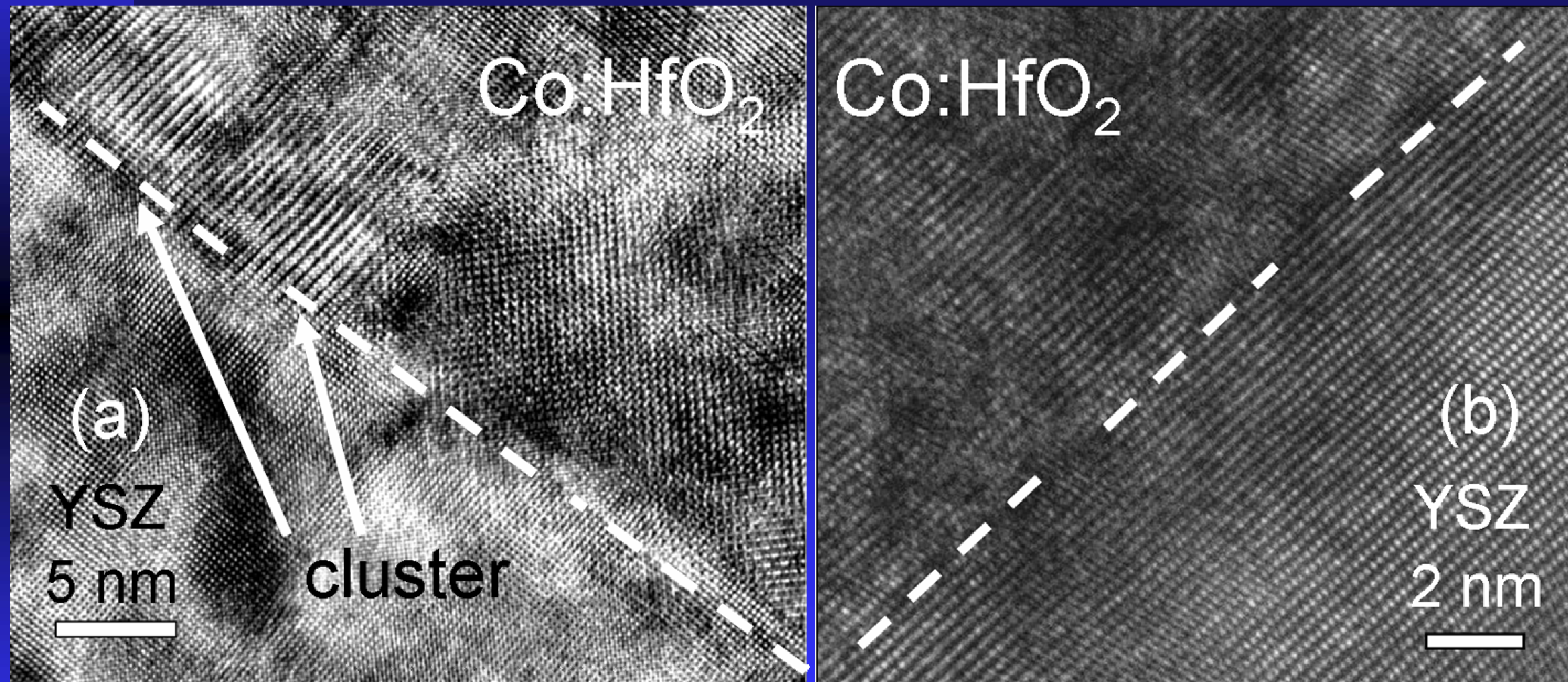

High-T (700°C) grown film
Monoclinic phase

Low-T (100°C) grown,
Polycrstalline film

EXAFS and Magnetic Characterization of High-T (700ºC) Grown Films

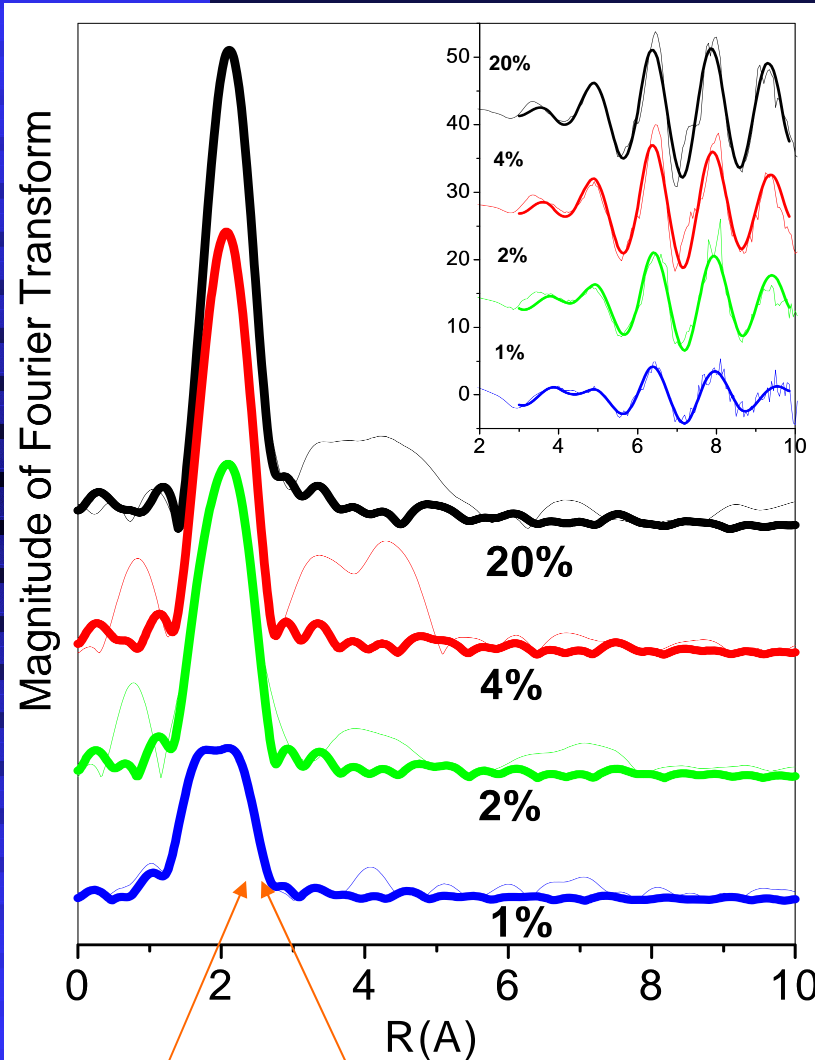

1st O shell + 2nd Co shell
2.04A 2.49A

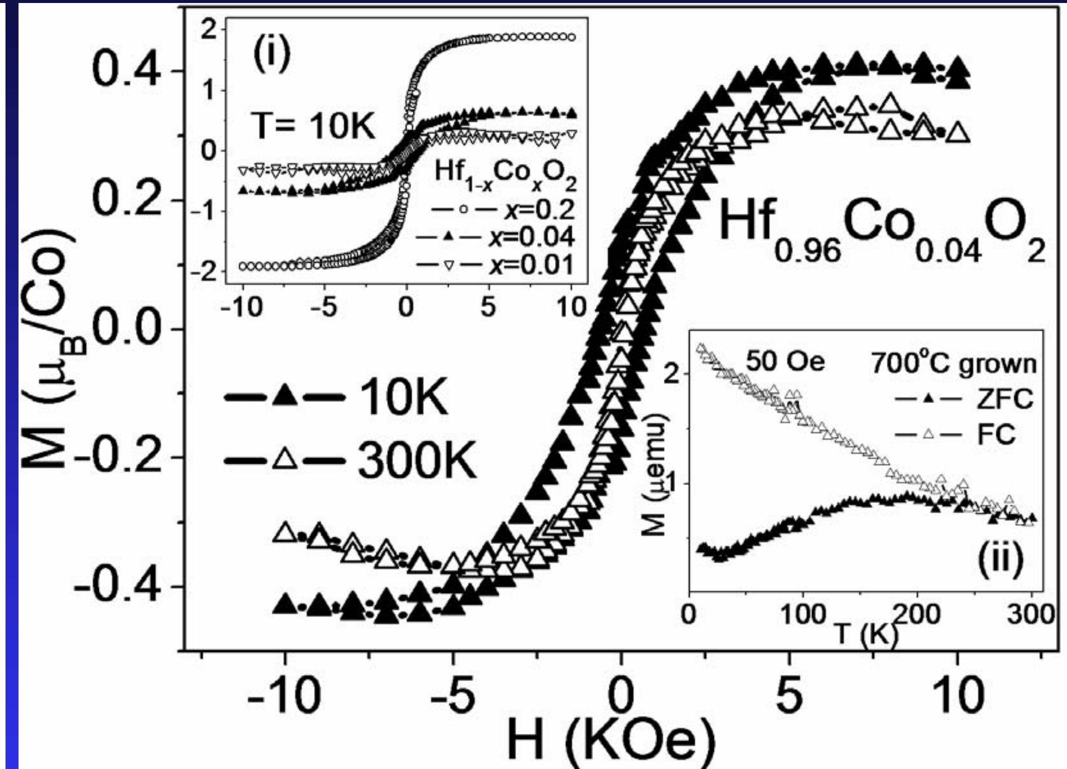

- EXAFS of the high-T grown samples showed a progressive formation of Co clusters in the film (Co = 1-20 at.%).
- **Superparramagnetic** temperature dependence.
- Saturation moment increases with increasing Co doping concentration.

Magnetic Property of Low-T Grown Films

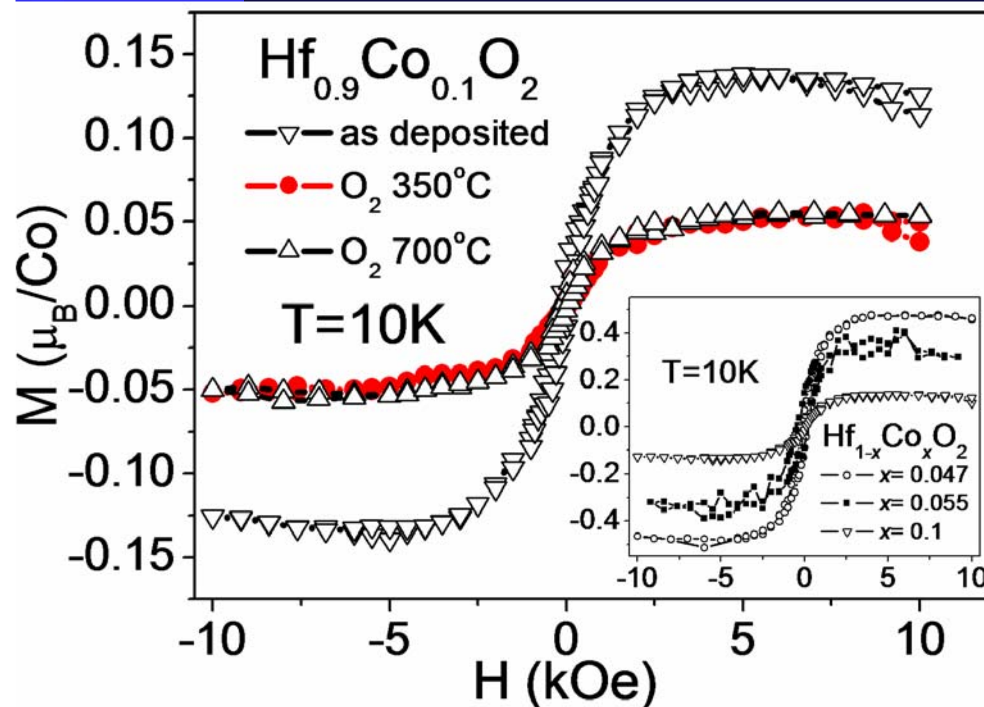

Substrate Temperature (℃)	40~100	40~100	40~100
Doping concentration (at.%)	4.7	5.5	10
Ms at 10K (μ_B/Co)	0.47	0.36	0.13
Ms at 300K(μ_B/Co)	0.43	0.29	0.1

- Ferromagnetic behavior was observed at both 10K and 300K.
- The magnetic moment decreases with increasing Co doping due to enhanced dopant dopant associations.
- The magnetic properties are stable after annealing in O_2 at 350°C.
- Correlation between saturation magnetization with concentrations of **oxygen vacancies**

F-center Exchange Mechanism:

--An electron orbital created by an **oxygen vacancy** with trapped electrons is expected to correlate with magnetic spins dispersed inside the oxides.

Impurity-band Exchange Model :

--The hydrogenic orbital formed by **donor defect (like oxygen vacancy)** associated with an electron overlaps to create delocalized impurity bands.

-- If the donor concentration is large enough and interacts with the magnetic cations with their 3d orbitals to form **bound magnetic polarons** leading to ferromagnetism.

$\gamma^3 \delta_p \approx 4.3$, **where** $\gamma = \varepsilon(m/m^*)$

δ_p **: polaron percolation threshold**

X_p **: cation percolation threshold**

γ_H **: hydrogenic radius**

M. Coey et al,
Nature Materials, 2005.

Theoretical Analysis Using Impurity Band Exchange Model

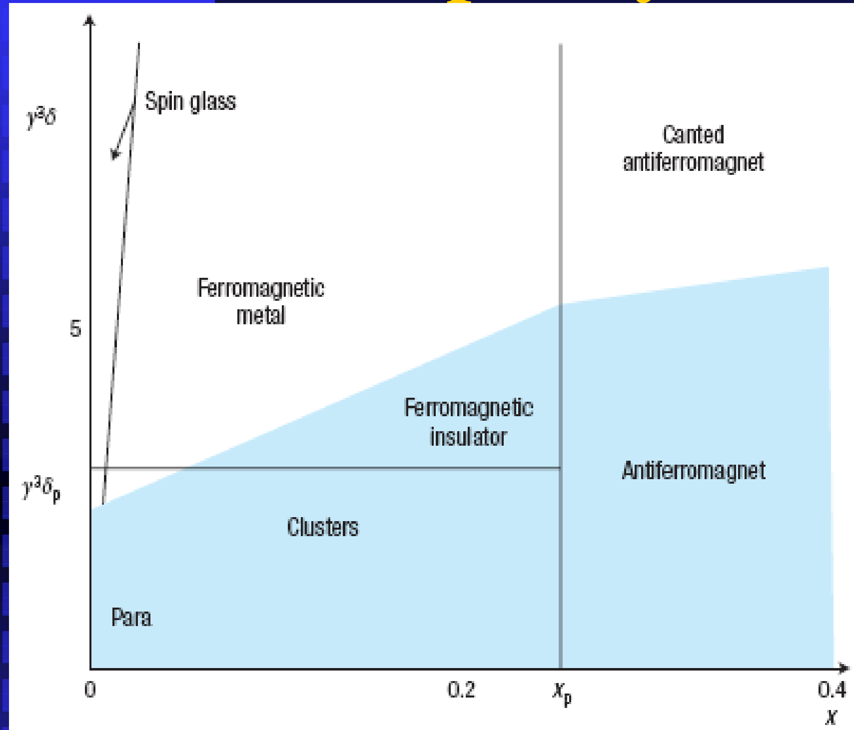

Material	ε	m^*/m	γ	γ_H (nm)	δ_P (10^{-6})
ZnO	4	0.28	14	0.76	1500
TiO_2	9	1	9	0.48	5900
SnO_2	3.9	0.24	16	0.86	1000
HfO_2	15	0.1	150	7.95	1.27
Al_2O_3	9	0.23	39	2.07	72

δ_p : Polaron percolation threshold
X_p : Cation percolation threshold
γ_H : Hydrogenic orbital radius

- δ_p and x_p are two landmarks on magnetic phase diagram.
- Ferromagnetism occurs when $\delta > \delta_p$ and $x < x_p$.
- δ_p of **HfO_2** based DMO is about **1.27×10^{-6} - 8.15×10^{-5}**
- Appearance of ferromagnetic insulator behavior in **HfO_2** is more likely than **ZnO, TiO_2** and **SnO_2** .
- Will try Y_2O_3, ZrO_2, and Al_2O_3 etc.

Major Research Topics

- Novel MBE template approach for ALD growth
- Enhancement of κ in the new phase through epitaxy
- Fundamental study by IETS for detections of phonons and defects in high κ dielectrics
- Room temperature ferromagnetism in cluster free, Co doped HfO_2 films

Acknowledgement

Co-PIs:

NTHU---Prof. M. Hong

NTHU---Prof. T. B. Wu

NTU---Prof. C. W. Liu

NCTU---Prof. A. Chin

Collaborators:

NSRRC---Dr. Chia-hong Hsu, Dr. H. Y. Lee

NTU/CCMS---Dr. M. W. Chu, Dr. S. C. Liou,
Dr. C. H. Chen

IOP/A.S.---Dr. S. F. Lee

NTHU---Prof. Y. L. Soo

Group Members：

何信佳博士、J. P. Mannaerts、吳彥達、李昆育、 李威縉、朱其新、李毅君、潘欽寒、徐雅玲、邱亦欣、黃建中、張宇行、洪宏宜 、游璇龍 、謝政義 + …etc

Acknowledgement :

Thanks to the Support of the NSC National Nano Project

HfO_2 High κ Dielectrics for III-V Compound Semiconductor Passivation And MOSFET

High κ Gate Oxide for High mobility channel Semiconductors like Ge and III-V semiconductors

The Quest for (III-V) MOSFETs

$GaGdO_x$ on GaAs

(1994-2007)

New High κ Dielectrics for GaAs Passivation

- Advantages of compound semiconductor
  - High electron mobility
  - Semi-insulating substrate
  - High breakdown field

- A key challenge of device processing
  - Surface passivation
  - Novel oxide of low density of state (D_{it}) and low leakage
  - MBE growth of **$Ga_2O_3(Gd_2O_3)$** of $\kappa = 12$ and **Gd_2O_3** of $\kappa = 14$.

Novel High κ Dielectrics for III-V Semiconductors

III-V Semiconductor Surface Passivation

Searching for an insulators with low D_{it} and low leakage

MOSFET's for high speed, high power, optoelectronic applications

--Discovery of a stable mixed oxide $Ga_2O_3(Gd_2O_3)$ deposited on **GaAs** with low D_{it}

-- Epitaxy of single crystal (110) Gd_2O_3 film on GaAs

-- Inversion-channel, E- and D-mode MOSFETs,

Have applied to other semiconductors such as InGaAs, AlGaAs, InP

Growth of $Ga_2O_3(Gd_2O_3)$ and (001)Gd_2O_3 on GaN

GaN/Gd_2O_3/GaN heteroepitaxy

Inventions toward GaAs MOSFET's at Bell Labs

- 1994
  - novel oxide $Ga_2O_3(Gd_2O_3)$ to effectively passivate GaAs surfaces
  - demonstration of low interfacial recombination velocities using PL
- 1995
  - establishment of accumulation and inversion in p- and n-channels in $Ga_2O_3(Gd_2O_3)$-GaAs MOS diodes with a low D_{it} of 2-3 x 10^{10} cm^{-2} eV^{-1}(IEDM)
- 1996
  - first e-mode GaAs MOSFETs in p- and n-channels with inversion (IEDM)
  - Thermodynamically stable
- 1997
  - e-mode inversion-channel n-InGaAs MOSFET with g_m= 190 mS/mm, and mobility of 470 cm^2/Vs (DRC, EDL)
- 1998
  - d-mode GaAs MOSFETs with negligible drain current drift and hysteresis (IEDM)
  - e-mode GaAs MOSFETs with improved drain current (over 100 times)
  - Dense, uniform microstructures; smooth, atomically sharp interface; low leakage currents
- 1999
  - GaAs power MOSFET
  - Single-crystal, single-domain Gd_2O_3 epitaxially grown on GaAs
- 2000
  - demonstration of GaAs CMOS inverter
- 2001-2002
  - Design of high-speed and high-power devices; reliability of devices

$Ga_2O_3(Gd_2O_3)$/GaAs Heterostructures

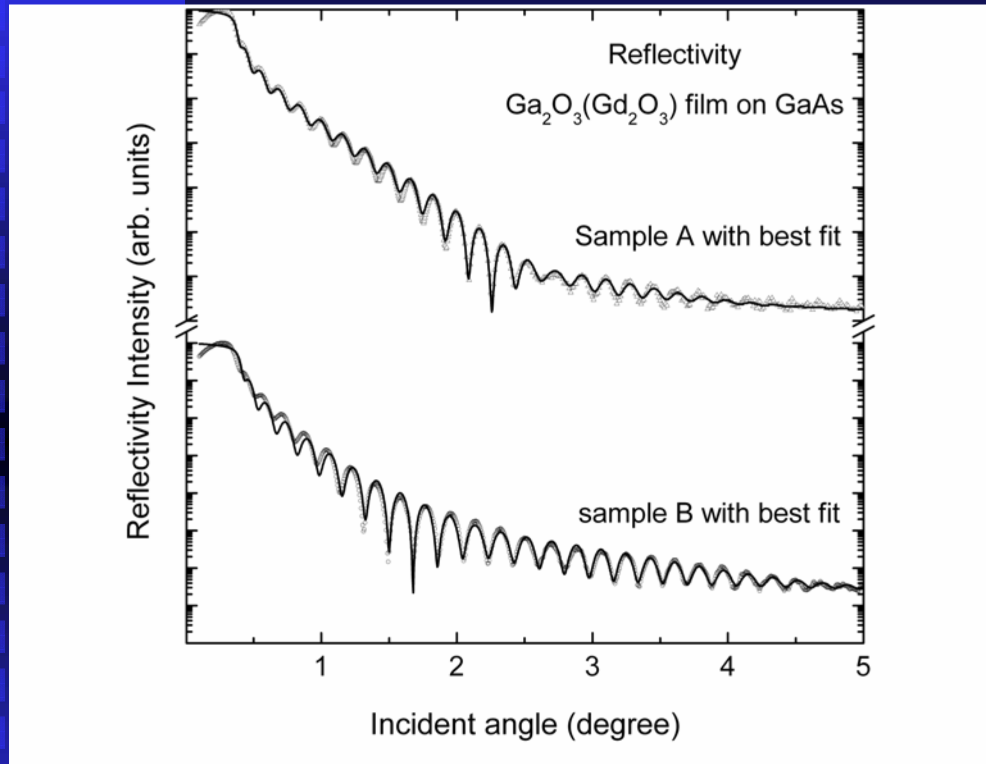

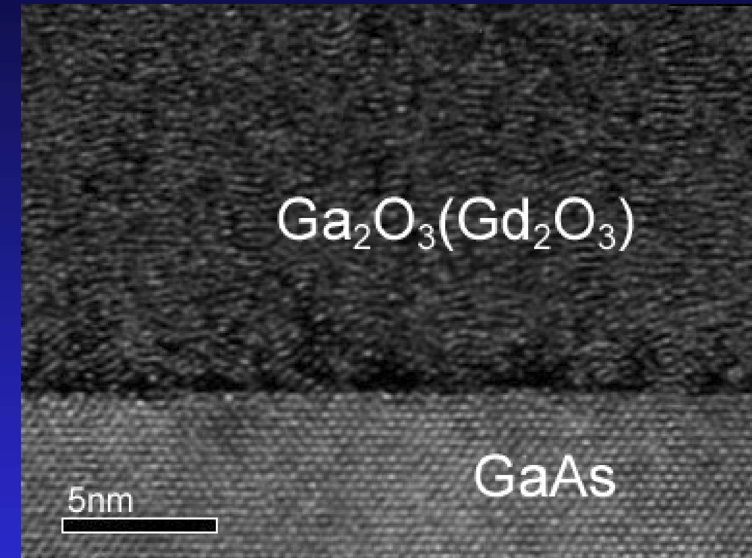

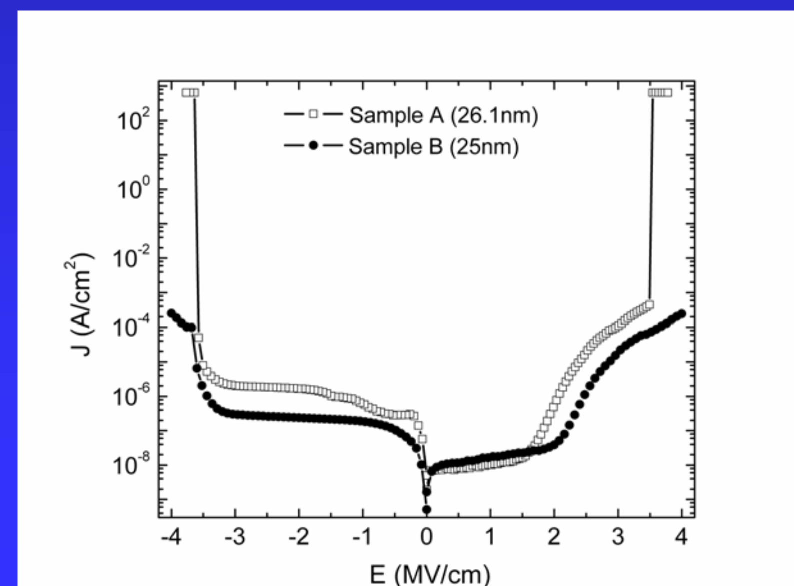

The oxide films remained amorphous with a sharp interface after 780°C anneal with $\kappa = 15$

D-mode GaAs/InGaAs MOSFET with $Ga_2O_3(Gd_2O_3)$ as a Gate Dielectric

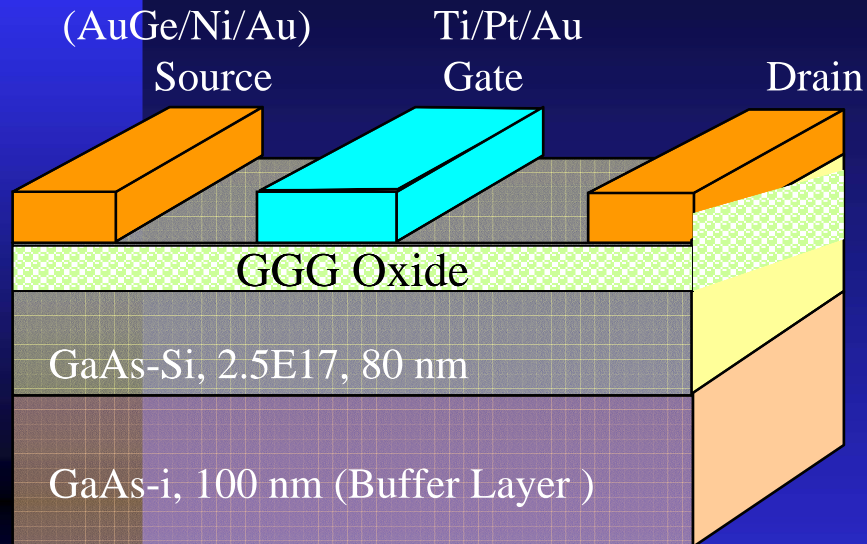

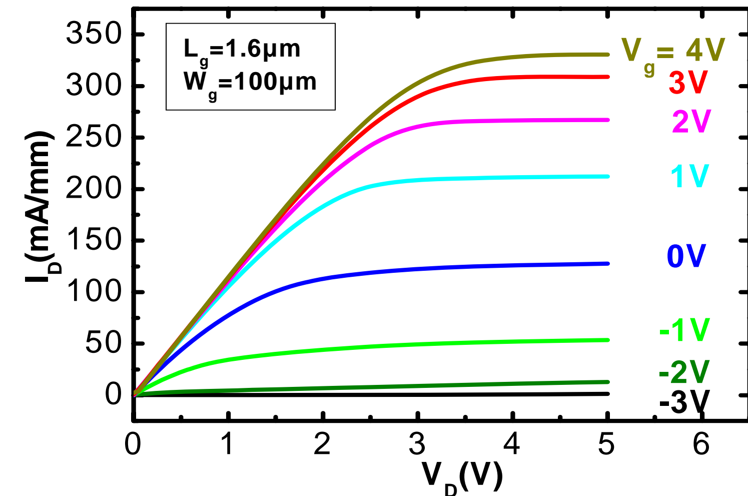

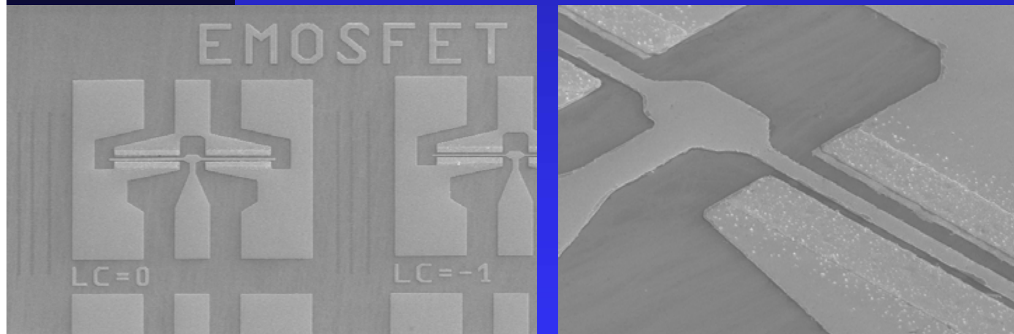

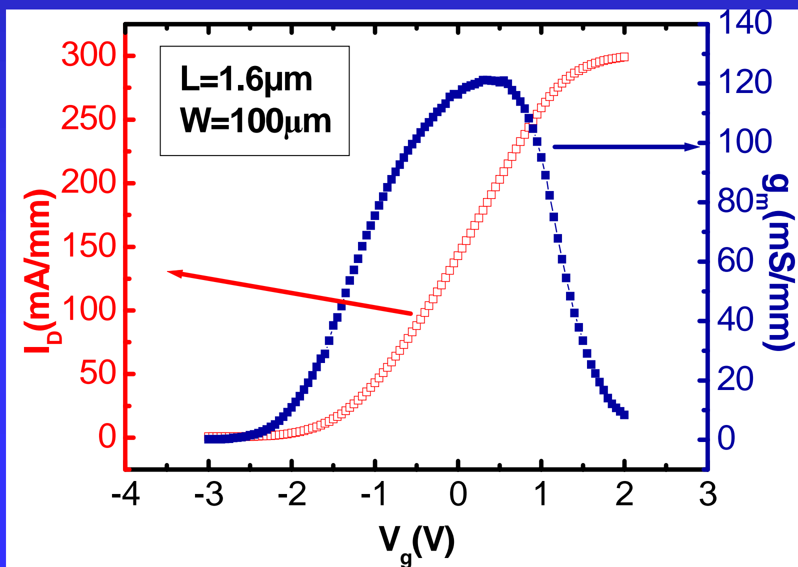

- 1.6 μm gate-length
- 335 mA/mm
- 120 mS/mm
- With $In_{0.15}Ga_{0.85}As$, 171 mS/mm

$Ga_2O_3(Gd_2O_3)$/InGaAs Oxide Scalability

MBE Growth , Al_2O_3 capping layer

- Al_2O_3/GGO(33nm)/$In_{0.2}Ga_{0.8}As$
- Al_2O_3/GGO(20nm)/$In_{0.2}Ga_{0.8}As$
- Al_2O_3/GGO(10nm)/$In_{0.2}Ga_{0.8}As$
- Al_2O_3/GGO(8.5nm)/$In_{0.2}Ga_{0.8}As$
- Al_2O_3/GGO(4.5nm)/$In_{0.2}Ga_{0.8}As$

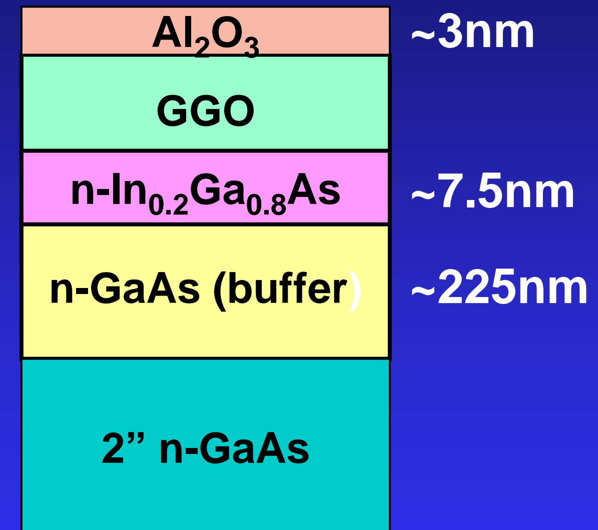

Electrical properties of Au/Al_2O_3/GGO/$In_{0.2}Ga_{0.8}As$/GaAs

N_2 800^{0}C 10 s + FG 375^{0}C 30 min

GGO thickness	κ value	ΔV_{FB}	Dispersion (10k-500k)	J@ V_{fb}+1V (A/cm^2)	D_{it} ($cm^{-2}eV^{-1}$)	GGO EOT
33nm	15-16	3.5V	2.8%	$1.18x10^{-9}$	$1.3x10^{11}$	8.3nm
20nm	14-15	1.3V	1.5%	$1.62x10^{-9}$	$1x10^{11}$	5.4nm
10nm	14-15	1.1V	2.2%	$1.46x10^{-9}$	$1.4x10^{11}$	2.7nm
8.5nm	14-15	1.1V	4.7%	$1.78x10^{-9}$	$2.6x10^{11}$	2.3nm
4.5 nm	14-15	1.1V	5.4%	$3.1 x 10^{-5}$	$1.3 x 10^{11}$	1.1 nm

- Al_2O_3 capping (3nm) effectively minimizing absorbing moisture in GGO.
- GGO (4.5nm) dielectric constant maintains at 14-15 (EOT~2.3nm).
- Larger flat band shift in thick GGO due to traps in GGO.
- D_{it}'s ~ low 10^{11}($cm^{-2}eV^{-1}$) range even subjected to 800°C annealing.

High κ Gate Oxide for High mobility channel Semiconductors like Ge

Surface cleaning 500˚C

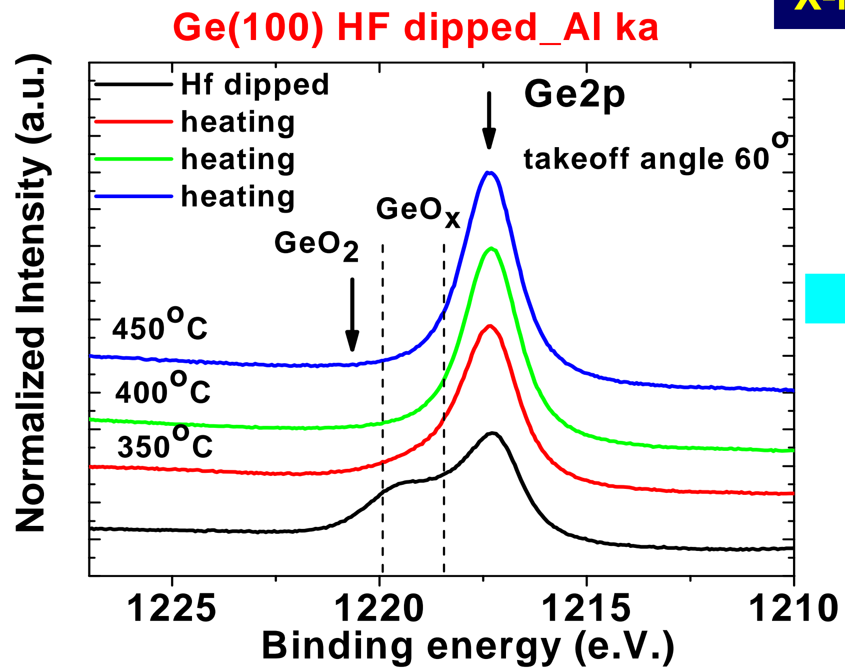

X-ray

Takeoff angle

Detector

Sample

108Å GGG
Ge substrate

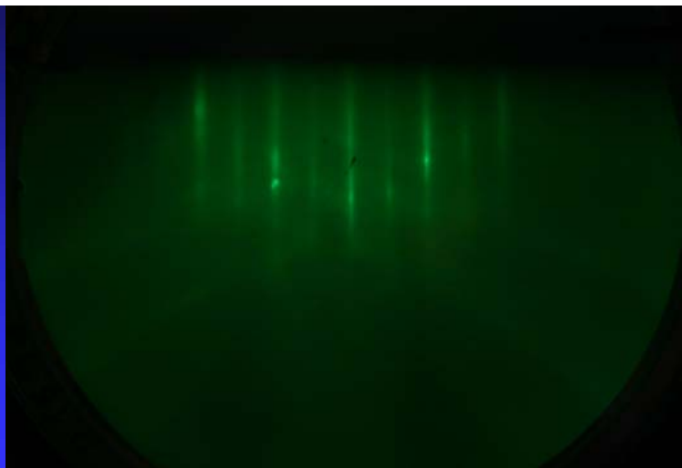

2X reconstruction

GGG growth temperature 500°C

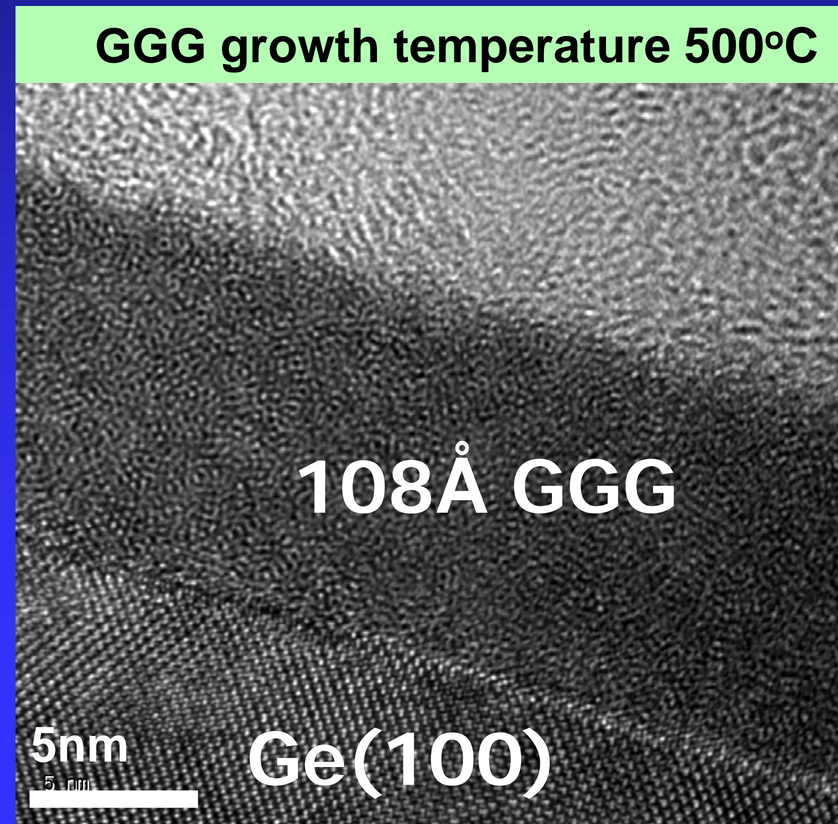

Structure Analysis of MBE GGG on Ge (100)

XPS **HRTEM** **RHEED**

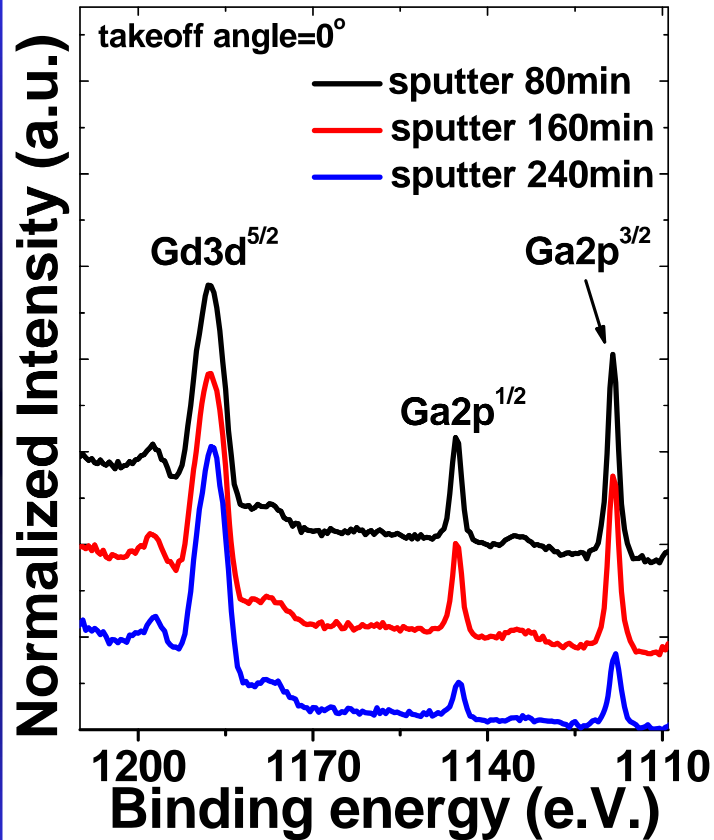

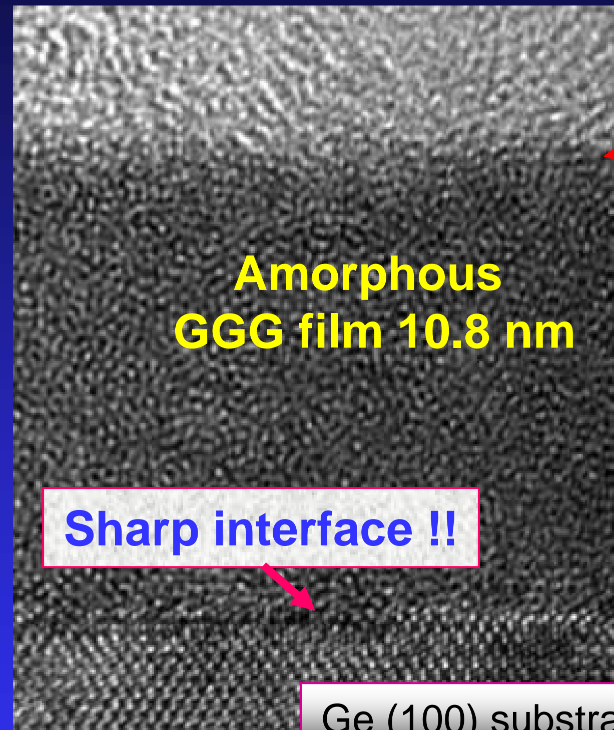

Amorphous GGG surface

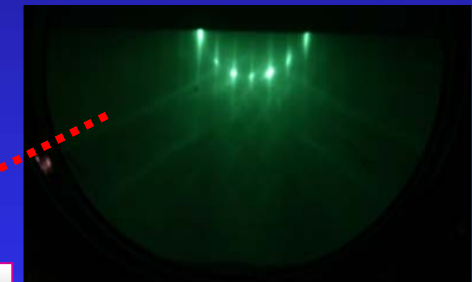

Atomically order 2X2 Ge(100) surface

(Depth analysis)

Less Gd_2O_3

More Gd_2O_3

MBE GGG

n-Ge (100)

Electrical Properties of GGG on Ge (100)

400°C 20min furnace annealing

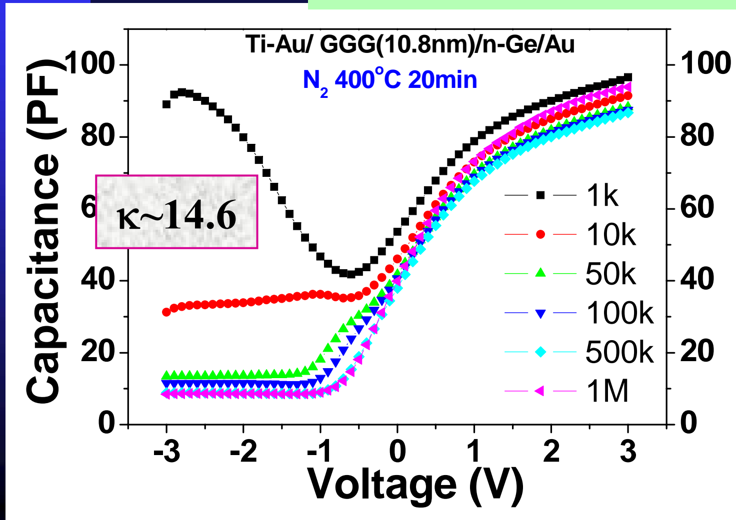

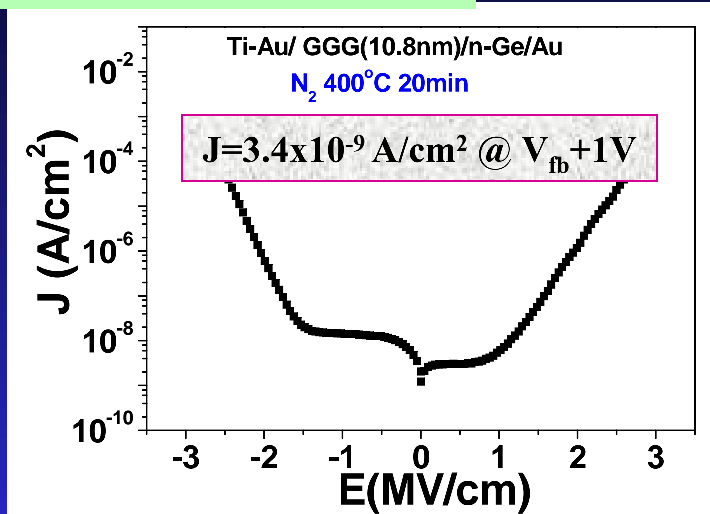

500°C 5min furnace annealing

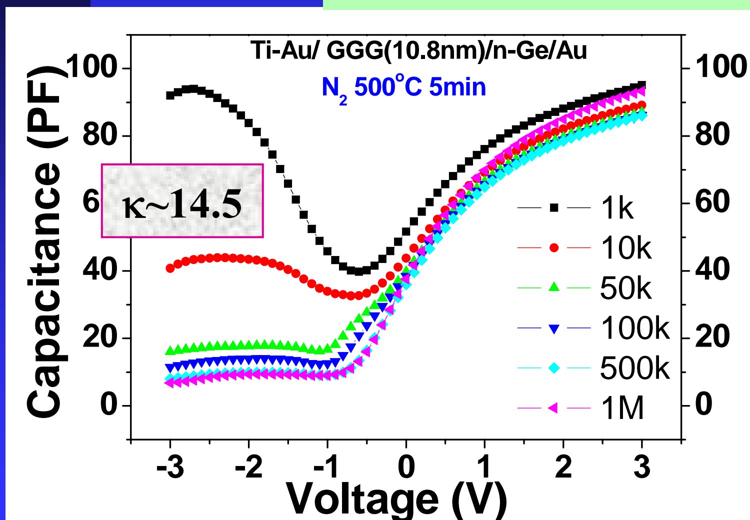

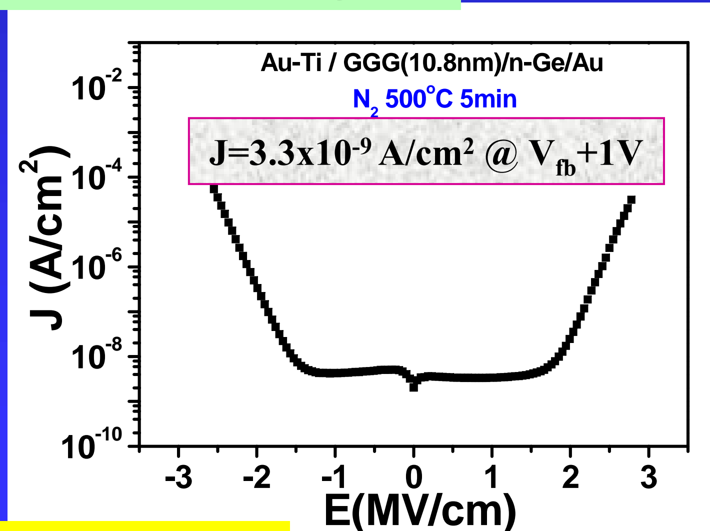

$D_{it}=1x10^{12}$ $cm^{-2}eV^{-1}$ @ midgap

Energy Band Diagram of as-grown GGG on Ge (100)

F-N Tunneling

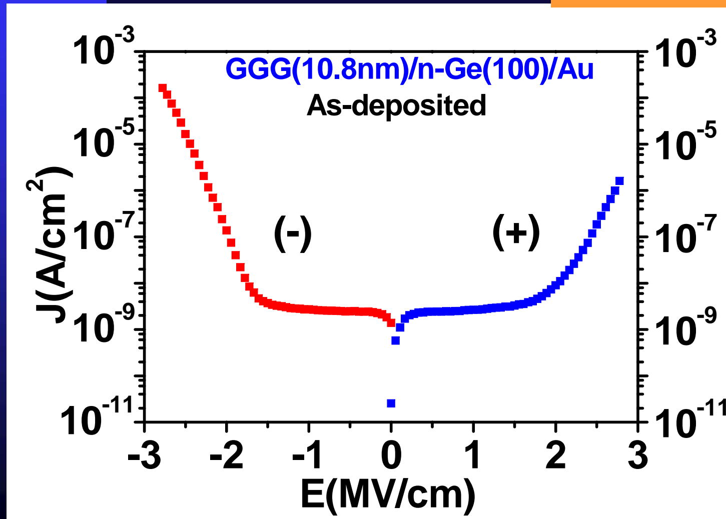

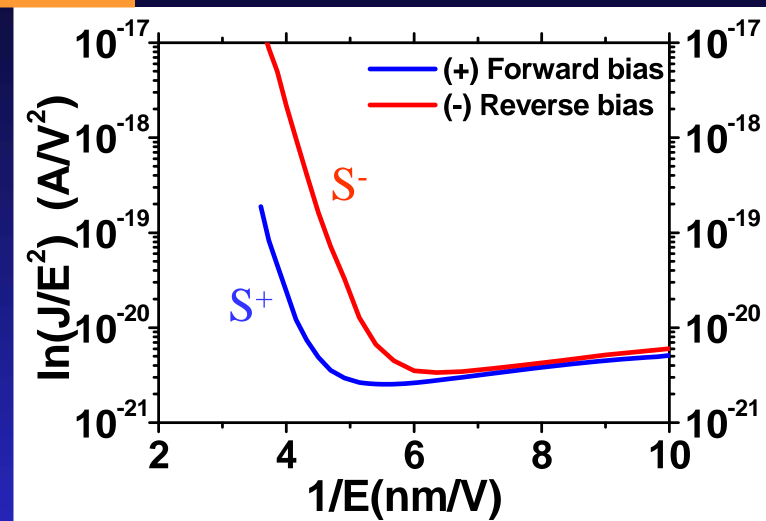

$J_{FN}=C(E_{ox})^2\exp(S/E_{ox}) \rightarrow \ln(J_{FN}/E_{ox}^2)=S/E_{ox}+\ln(C)$

$S = -8\pi(2m^*/m_e)^{1/2}(\varphi)^{3/2}/3qh$

$= -6.83\times10^7 (m^*/m_e)^{1/2}(\varphi)^{3/2}$

$(\varphi^- - \varphi^+) = (\Phi_m - X_S) = 0.8$ ------ (1)

$2.78 = (m^*/m_e)^{1/2}(\varphi^-)^{3/2}$ ------ (2)

$1.75 = (m^*/m_e)^{1/2}(\varphi^+)^{3/2}$ ------ (3)

$\varphi^+ = \Delta E_C = 2$ eV

$m^* = 0.3m_e$

$\varphi^- = 2.8$eV

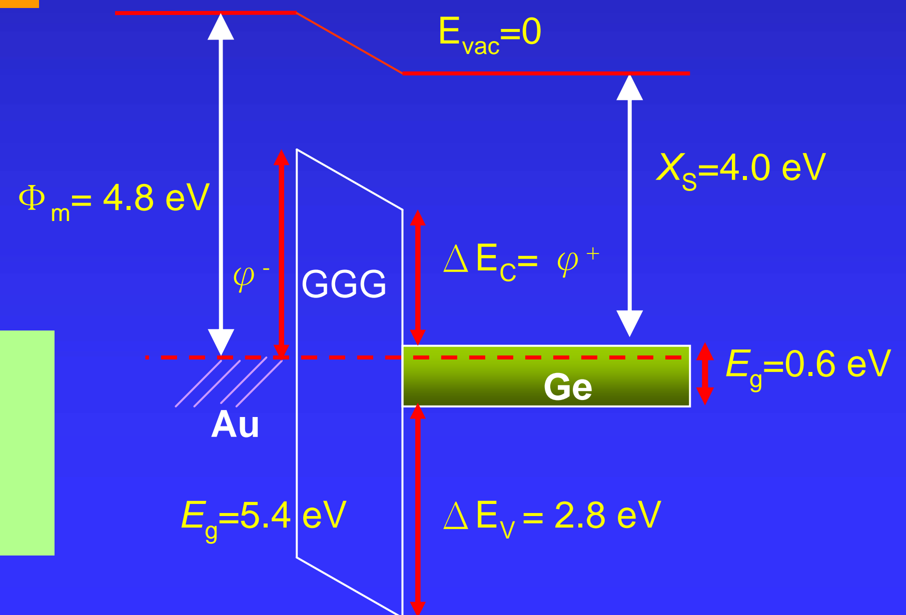

[2]. T.S.Lay, et. al. Solid state electronics **45,** 1679 (2001).